Review of Palaeobotany and Palynology 178 (2012) 43–58

Contents lists available at SciVerse ScienceDirect

Review of Palaeobotany and Palynology

journal homepage: www.elsevier.com/locate/revpalbo

Research paper

Phytolith signal of aquatic plants and soils in Chad, Central Africa

Alice Novello [a,b,*], Doris Barboni [b], Laure Berti-Equille [b,c], Jean-Charles Mazur [b], Pierre Poilecot [d], Patrick Vignaud [a]

[a] IPHEP, Institut International de Paléoprimatologie, Paléontologie Humaine: Evolution et Paléoenvironnements, UMR 7262 CNRS-INEE, Université de Poitiers, UFRSFA, 40 avenue du Recteur Pineau, 86022 Poitiers cedex, France
[b] CEREGE, Centre Européen de Recherche et d'Enseignement des Géosciences de l'Environnement, UMR 7330 Aix-Marseille Université – CNRS – IRD, BP80, F-13545 Aix-en-Provence cedex 4, France
[c] IRD, Institut de Recherche pour le développement, UMR ESPACE DEV, Maison de la Télédétection, 500 avenue Jean-François Breton, F-34093 Montpellier cedex 5, France
[d] CIRAD, Centre de coopération International en Recherche Agronomique pour le Développement, Département ES, UR AGIRs, TA C 22/E, Campus International de Baillarguet, 34398 Montpellier cedex 5, France

ARTICLE INFO

Article history:
Received 10 June 2011
Received in revised form 21 March 2012
Accepted 27 March 2012
Available online 6 April 2012

Keywords:
Poaceae
Cyperaceae
lacustrine environments
Lake Chad
silica
Sub-Sahara

ABSTRACT

To identify the phytolith signal of lacustrine environments, which are prone to preserving faunal remains including hominins, we analyzed the phytolith content of 46 grass and sedge species, and of 26 soil and mud samples. The samples were collected in Chad (Central Africa), in the Sudanian and Sahelian phytogeographical zones, near temporary and permanent water-bodies (including Lake Chad) and in grass-dominated biomes on well-drained soils. Altogether, we observed and counted separately 80 different phytolith types, including 38 grass silica short cells (GSSCs). Phytolith type diversity and relative abundances were analyzed in the botanical specimens to improve the phytolith taxonomic resolution. For the Poaceae, we used a value-test analysis to identify significant cohorts of phytoliths to characterize aquatic, mesophytic, and xerophytic species. Our results show that the abundance of Cyperaceae in swampy areas may be deduced from the combined abundance of blocky and elongate phytolith types, but not by the typical silicified Papillae phytoliths, which were barely found preserved in the soil/mud. The abundance of aquatic Poaceae near water-bodies is inferred from the presence and abundance of a cohort of eight GSSC types (including notably several trapeziform GSSCs within the bilobate, cross, and saddle categories), which averages 42% in the mud samples, but only 23% and 14% in the samples from the Sudanian and Sahelian zones, respectively. The characterization is unclear for mesophytic grasses, but obvious for xerophytic grasses whose abundance in the Sahelian grasslands is inferred from the presence and abundance of a cohort of five GSSC types (mainly tabular saddles), which averages 50% in the soil samples from the arid Sahelian zone, and <19% in the more humid Sudanian and swamp samples. In conclusion, considering the full morphological diversity of grass silica short cell phytoliths (rather than just the broad morphological categories) allows greater discrimination of the aquatic environments. Such approach is therefore required for analyzing vegetation distribution at a local scale.

1. Introduction

Lacustrine and fluviatile environments are known to be highly favorable for the preservation of faunal fossil remains, including hominin remains (e.g. Vignaud et al., 2002; WoldeGabriel et al., 2009). In the past two decades, more than 18,000 faunal specimens including fossils of *Sahelanthropus tchadensis*, the earliest hominin known thus far dated (ca 7 Ma) (Brunet et al., 2002; Vignaud et al., 2002; Brunet et al., 2005; Lebatard et al., 2008), and *Australopithecus bahreghazali* (ca 3.58 Ma) (Brunet et al., 1995; Brunet et al., 1996; Lebatard et al., 2010), were discovered in the Toros-Menalla and Koro-Toro fossiliferous areas in the northern part of Lake Chad basin. Earlier in the 1960s, some silicified woody elements were also found at several Mio–Pliocene localities, between 15 and 22°N (Coppens and Koeniguer, 1976). These elements include a liana of extant Caesalpiniaceae, large tree trunks (one up to 17 m long and 60 cm diameter) attributed to Mimosaceae, and other remains attributed to various extant families such as Sapindaceae, Rubiaceae, Moraceae and Tamaricaceae. This paleoflora suggests Sahelian and Sudanian vegetation types and climate sometime during the Mio–Pliocene. Other approaches using for example dental mesowears (Blondel et al., 2010), faunal assemblages (e.g. LeFur et al., 2009; Otero et al., 2010), stable isotopes of teeth-enamel (e.g. Zazzo et al., 2000), or sedimentology (Schuster, 2002) also indicate the presence of mosaic environments from grasslands to woodlands, with the presence of swampy areas in the northern part of Chad basin during the Mio–Pliocene. Recent ongoing sedimentological investigations suggest that it is possible to further improve the Mio–Pliocene paleoenvironmental reconstructions of the Chad basin through the

* Corresponding author at: CEREGE, BP80, F-13545 Aix-en-Provence cedex 4, France. Tel.: +33 4 42 97 17 58; fax: +33 4 42 97 17 40.
E-mail address: alice.novello@univ-poitiers.fr (A. Novello).

0034-6667/$ – see front matter © 2012 Elsevier B.V. All rights reserved.
doi:10.1016/j.revpalbo.2012.03.010

investigation of plant phytoliths, which were found abundant and well preserved in many geological levels with fossil vertebrate (Barboni and Novello, unpublished data).

Phytoliths are micro-botanical particles (2–200 μm) produced by many terrestrial plants (Piperno, 2006). They are most distinctive among grasses (Poaceae), some domesticated plants, and several other botanical families (Piperno, 2006). Several modern soil studies in Africa showed that phytolith assemblages are reliable vegetation and climate proxies. For example, the relative abundance of grass silica short cells (Poaceae) versus forest indicator phytoliths (mainly globular silica bodies) are used to estimate the vegetation tree cover at low and mid-elevation (Alexandre et al., 1997; Bremond et al., 2005; Barboni et al., 2007; Bremond et al., 2008b). Phytolith assemblages record other aspects of the vegetation such as the relative abundance of short versus tall grasses, which may be interpreted in terms of annual precipitation and water availability (Bremond et al., 2004). In West Africa, if most studies focused on the potential for phytolith assemblages to characterize vegetation zones and climatic gradients at the regional scale (Alexandre et al., 1997; Bremond et al., 2004, 2005; Barboni et al., 2007; Bremond et al., 2008a, 2008b), recent work in Mali has dealt with the potential of phytolith assemblages to characterize local environments at archeological sites (Neumann et al., 2009). This last approach, which requires advanced morphological discrimination of the phytoliths, exploits the great morphological variability of grass silica short cells and other mono- and dicotyledonous phytoliths to identify environmental parameters or improve taxonomical identification of plants (Fahmy, 2008; Barboni and Bremond, 2009; Mercader et al., 2009; Eichhorn et al., 2010; Mercader et al., 2010).

Considering these two different approaches, we carried out a phytolith study of the aquatic vegetation of present-day Lake Chad, as well as of temporary aquatic grasslands and swamps in Chad. The aim of this study is to determine if it is possible to distinguish aquatic from non-aquatic environments based on the phytolith assemblages preserved in the soils. What is the phytolith signal of the water-loving plants associated with the permanent and temporary water bodies in Chad? Are the phytoliths of these helo- and hydrophytic plants well represented in the soils? Is the phytolith signal of permanent aquatic environments remarkable despite the phytolith redundancy?

2. Environmental settings

Chad is characterized by a strong south to north gradient of increasing aridity. South of 11°N, mean annual precipitation is >800 mm/yr and dry season is <8 months, while north of 14°N, mean annual precipitation is <200 mm/yr and dry season >9–10 months (Lézine et al., 2009). The precipitation regime strongly influences the diversity of landscapes and the regional distribution of vegetation. In Chad, three main phytogeographical zones are distributed from south to north (White, 1983) (Fig. 1). The humid Sudanian zone is covered by undifferentiated woodlands or woodlands with abundant *Isoberlinia* in the south. This zone is more wooded than the Sahelian zone occurring further north, which is covered by wooded grasslands and deciduous bushlands. Yet, both the Sudanian and the Sahelian zones include large "pockets" of grassland mosaics with *Acacia* wooded grasslands, so-called edaphic grasslands. The Saharan zone, which occurs north of 14°N, is almost devoid of vegetation at low altitude (White, 1983) (Fig. 1). Along the south to north gradient of increasing aridity, the height of grasses decreases from 100 to 200 cm in the Sudanian zone, to less than 50 cm in the Sahelian zone (Schmidt et al., 2011). Our field observations indicate that the Panicoideae grasses dominate in the humid south, and Chloridoideae and Aristidoideae dominate in the arid north.

Present-day Lake Chad occupies a large depression (25,000 km^2 in the 1960s, but <1500 km^2 in 2000s) (UNEP, 2004). It is located in the Sahelian phytogeographical zone, at the edge of the Saharan desert and is almost exclusively supplied by the Chari-Logone river system draining the humid tropics (Fontes et al., 1970) (Fig. 1). Precipitation, which is highly variable from one year to the other strongly influences lake level fluctuations (Lemoalle and Hourtal, 1996) and vegetation composition and distribution near the lake (Fotius and Lemoalle, 1976; Gaston and Dulieu, 1976). Vegetation associated to Lake Chad is essentially aquatic with abundant herbaceous species from the Poaceae

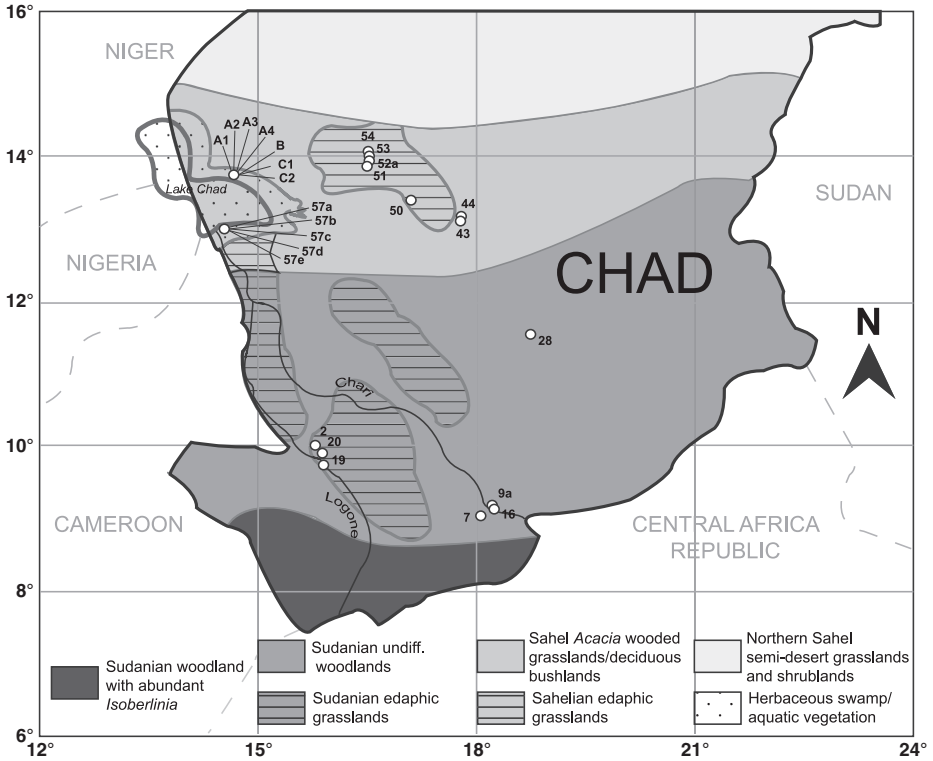

Fig. 1. Location of the soil/mud samples in Chad (Central Africa) and main phytogeographic zones after White (1983).

(essentially the helo- and hydrophytic *Phragmites australis*, *Vossia cuspidata*, *Echinochloa pyramidalis* and *Leersia hexandra*), Cyperaceae (mainly *Cyperus papyrus* and *Cyperus articulatus*) and Typhaceae (*Typha domingensis*) in association with some other aquatics such as the tree *Aeschynomene elaphroxylon* and the Convolvulaceae *Ipomoea aquatica*. Vegetation on the emerged dunes, however, includes various *Acacia* species, the palm *Hyphaene thebaica*, and xerophytic grasses such as *Cenchrus biflorus* and *Panicum turgidum* (Gaston and Dulieu, 1976; Gaston, 1996; Olivry et al., 1996).

3. Material and methods

To identify the phytolith signal of the aquatic plants and vegetation types associated with permanent and temporary water bodies in Central Africa, we analyzed the phytolith content of 26 mud and surface soil samples, and 46 plant samples collected at various locations in Chad between 9°N and 14°N (Table 1, Fig. 1). At Lake Chad location we collected mud samples directly from aquatic swamps and grasslands in the Bol archipelago in the north (samples B, A1 to A4), and near the locality of Karal in the south (samples 57a to 57e). At Bol, not far from the lakeshore we collected two additional samples on a dune with Acacias and *Hyphaene thebaica* (samples C1, C2). Seven other samples were collected in the Sahelian zone, three in temporary swamps (samples 54, 53, 50) and four in *Acacia* wooded grasslands and shrub steppes (samples 52a, 51, 44, 43). We collected another set of seven samples in the Sudanian zone, four in temporary aquatic grasslands (samples 2, 20, 19, 16), and three in tree savannas and woodlands (samples 28, 9a, 7) (Fig. 1).

At each sampling site we made an inventory of the most abundant plants (Table 1), and collected every herbaceous Poaceae and Cyperaceae species that was not already available in the CIRAD herbarium at Montpellier (France). Ten Poaceae and two Cyperaceae species that were not observed in the field, but documented from the Sahelian and Sudanian zones in Chad (César and Lebrun, 2003), were also sampled from the herbarium and included in this study. In total, our dataset includes 46 herbaceous species including eight Cyperaceae, 37 Poaceae, and the Typhaceae *Typha domingensis* (Table 2). Almost half of the dataset is made of hydrophytes (real aquatic plants) and helophytes (marsh plants). Hereafter, helo- and hydrophytes will be referred to as aquatics.

Table 1
Surface soil samples collected in Chad, with species inventories at the sampling sites.

ID	Coordinates	Plant associations/most abundant species	Vegetation physiognomy (Boughey, 1957)
Sahelian edaphic grassland mosaics with *Acacia* wooded grassland (unit 62)			
54	13°55′18″N, 16°29′00″E, 297 m (a.s.l.)	*Acacia nilotica*, *Cordia sinensis*, *Blumea cf. adamsii*, *Cyperus longus*, *Cyperus difformis*	Closed *Acacia* temporary herb-swamp
53	13°50′46″N, 16°29′25″E, 295 m	*Acacia nilotica*, *Cordia sinensis*, *Schoenoplectus roylei*, *Glinus lotoides*, *Sphenoclea zeylanica*, *Cyperus difformis*	
52a	13°47′31″N, 16°28′40″E, 314 m	*Acacia tortilis*, *Eragrostis tremula*, *Aristida mutabilis*, *Panicum turgidum*, *Cenchrus biflorus*, *Boerhavia repens*	Tree and shrub steppe
51	13°46′34″N, 16°28′30″E, 301 m	*Cordia sinensis*, *Acacia mellifera*, *Panicum laetum*, *Dactyloctenium aegyptium*, *Eragrostis pilosa*, *Boerhavia repens*	Dwarf-shrub steppe
50	13°16′56″N, 16°55′55″E, 305 m	*Acacia nilotica*, *Cyperus longus*, *Nymphaea lotus*	Closed *Acacia* temporary herb-swamp
Sahel *Acacia* wooded grasslands and deciduous bushlands (unit 43)			
44	13°03′47″N, 17°44′09″E, 319 m	*Calotropis procera*, *Schoenefeldia gracilis*, *Schizachyrium exile*, *Aristida mutabilis*	Grass savanna
43	13°01′30″N, 17°43′40″E, 318 m	*Indigofera oblongifolia*, *Schoenefeldia gracilis*, *Eragrostis tremula*, *Panicum laetum*, *Spermacoce radiata*	Tree and shrub savanna
Sahelian herbaceous swamp and aquatic vegetation (Lake Chad) (unit 75)			
C1	13°25′51″N, 14°44′03″E, 283 m	*Acacia nilotica*, *Acacia senegalensis*, *Hyphaene thebaica*, *Cenchrus biflorus*, *Dactyloctenium aegyptium*, *Panicum turgidum*	Tree and shrub steppe
C2	13°25′51″N, 14°44′03″E, 283 m		
B	13°26′03″N, 14°44′13″E, 275 m	Lake Chad archipelago (north)	Aquatic grassland and herb swamp
A3	13°25′23″N, 14°44′55″E, 277 m	*Aeschynomene elaphroxylon*, *Ipomoea aquatica*, *Typha domingensis*, *Phragmites australis*, *Vossia cuspidata*, *Echinochloa pyramidalis*, *Leersia hexandra*, *Cyperus articulatus*, *Cyperus papyrus*	
A4	13°25′23″N, 14°44′55″E, 277 m		
A1	13°25′07″N, 14°45′25″E, 269 m		
A2	13°25′07″N, 14°45′25″E, 269 m		
57e	12°56′39″N, 14°35′44″E, 298 m	Lake Chad (south)	
57d	12°55′47″N, 14°36′42″E, 300 m	*Aeschynomene elaphroxylon*, *Ipomoea aquatica*, *Typha domingensis*, *Phragmites australis*, *Vossia cuspidata*, *Echinochloa pyramidalis*, *Leersia hexandra*, *Cyperus articulatus*	
57c	12°55′11″N, 14°37′39″E, 299 m		
57b	12°54′49″N, 14°37′45″E, 312 m		
57a	12°54′41″N, 14°37′46″E, ?[a] m		
Sudanian edaphic grassland mosaics with communities of Acacia and broad-leaved trees (unit 63)			
2	9°59′26″N, 15°42′18″E, 360 m	*Vetiveria nigritana*, *Setaria sphacelata*, *Panicum fluviicola*, *Brachiaria jubata*[b], *Leersia hexandra*	Temporary aquatic grassland
20	9°53′41″N, 15°47′56″E, 355 m	*Vetiveria nigritana*, *Eragrostis squamata*, *Brachiaria jubata*[b], *Acroceras ampectens*, *Setaria sphacelata*	
19	9°44′03″N, 15°48′43″E, 357 m	*Vetiveria nigritana*, *Echinochloa pyramidalis*, *Oryza longistaminata*, *Panicum fluviicola*, *Eragrostis squamata*, *Acroceras amplectens*, *Brachiaria jubata*[b], *Setaria sphacelata*, *Pycreus macrostachyos*	
Sudanian undifferentiated woodlands (unit 29a)			
28	11°31′34″N, 19°10′32″E, 553 m	*Anogeissus leiocarpa*, *Sclerocarya birrea*, *Balanites aegyptiaca*, *Hyparrhenia bagirmica*, *Andropogon gayanus*	Tree savanna
9a	9°11′33″N, 18°11′49″E, 367 m	*Mitragyna inermis*, *Daniellia oliveri*, *Terminalia schimperana*, *Acacia sieberiana*, *Combretum collinum*, *Panicum anabaptistum*, *Vetiveria nigritana*, *Sporobolus cordofanus*, *Desmodium adscendens*	Woodland
16	9°10′50″N, 18°07′59″E, 370 m	*Acacia sieberiana*, *Piliostigma thonningii*, *Oryza longistaminata*, *Eragrostis squamata*, *Setaria sphacelata*, *Loudetia simplex*, *Panicum subalbidum*, *Pycreus macrostachyos*	Temporary aquatic grassland
7	9°04′55″N, 18°03′32″E, 434 m	*Anogeissus leiocarpa*, *Khaya senegalensis*, *Prosopis africana*, *Cassia obtusifola*, *Chamaecrista mimosoide*, *Digitaria ciliaris*	Tree savanna

[a] Missing data.
[b] Species replaced with *Brachiaria xantholeuca* for phytolith extraction.

Table 2
Plant species collected in Chad or sampled from the CIRAD herbarium (Montpellier, France), along with species photosynthetic pathway and water-requirement. Hy: hydrophytic, He: Helophytic, Me: mesophytic, Xe: xerophytic.

Family and subfamily	Species	C3/C4	Sampling area	Water-Requirement
Cyperaceae	*Cyperus alopecuroides Rottb.*	C3	Herbarium specimen no. 42216	Hy
	Cyperus articulatus L.	C4	13°19′11″N, 14°47′20″E, 274 m	Hy
	Cyperus difformis L.	C3	11°48′12″N, 15°12′50″E, 318 m	He
	Cyperus longus L.	C3	13°16′56″N, 16°55′55″E, 305 m	Hy/He
	Cyperus papyrus[a] *L.*	C4	13°25′23″N, 14°44′55″E, 277 m	Hy
	Cyperus pustulatus Vahl	C3	9°13′28″N, 18°07′55″E, 375 m	He
	Pycreus macrostachyos (Lam.) J. Raynal	C3	Herbarium specimen no. 6394	He
	Schoenoplectus roylei (Nees) Ovczinn & Czukav.	C3	Herbarium specimen no. 1614	He
Poaceae				
Aristidoideae	*Aristida mutabilis Trin. & Rupr.*	C4	Herbarium specimen no. 7323	Xe
	Aristida stipoides Lam.	C4	Herbarium specimen no. 3958	Xe
Arundinoideae	*Phragmites australis (Cav.) Trin.*	C3	13°25′07″N, 14°45′25″E, 269 m	Hy
Chloridoideae	*Chloris pilosa Schumach.*	C4	Herbarium specimen no. 4491	Xe
	Ctenium elegans Kunth	C4	Herbarium specimen no. 3961	Xe
	Cynodon dactylon (L.) Pers.	C4	Herbarium specimen no. 5233	Xe
	Dactyloctenium aegyptium (L.) Willd.	C4	Herbarium specimen no. 7114	Xe
	Eragrostis pilosa (L.) P. Beauv.	C4	Herbarium specimen no. 7306	Xe
	Eragrostis squamata (Lam.) Steud.	C4	9°10′50″N, 18°07′59″E, 370 m	He
	Eragrostis tremula Steud.	C4	Herbarium specimen no. 17657	Xe
	Schoenefeldia gracilis Kunth	C4	Herbarium specimen no. 7253	Xe
	Sporobolus cordofanus (Steud.) Coss.	C4	11°31′34″N, 19°10′32″E, 553 m	Me
Ehrhartoideae	*Leersia hexandra Swarts*	C3	13°26′02″N, 14°44′E, 271–272 m	Hy
	Oryza longistaminata A. Chev. & Roehr.	C3	Herbarium specimen no. 6732	Hy/He
Panicoideae	*Acroceras amplectens Stapf*	C3	Herbarium specimen no. 7900	He
	Andropogon gayanus Kunth (var. gayanus)	C4	Herbarium specimen no. 6764	Me
	Andropogon pseudapricus Stapf	C4	Herbarium specimen no. 7890	Me
	Brachiaria xantholeuca[b] *(Schinz) Stapf*	C4	Herbarium specimen no. 7307	Xe
	Cenchrus biflorus Roxb.	C4	13°25′51″N, 14°44′03″E, 283 m	Xe
	Digitaria ciliaris[a] *(Retz.) Koeler*	C4	10°36′27″N, 15°34′00″E, 328 m	Me
	Diheteropogon amplectens (Nees) Clayton	C4	Herbarium specimen no. 7730	Me
	Echinochloa pyramidalis (Lam.) Hitchc. & Chase	C4	Herbarium specimen no. 10455	Hy
	Hyparrhenia bagirmica (Stapf) Stapf	C4	Herbarium specimen no. 7766	Me
	Hyparrhenia barteri (Hack.) Stapf	C4	9°10′43″N, 17°47′17″E, 439 m	Me
	Hyperthelia dissoluta (Nees ex Steud.) Clayton	C4	Herbarium specimen no. 42952	Me
	Loudetia simplex (Nees) Hubb.	C4	Herbarium specimen no. 6757	Me
	Loudetia togoensis (Pilg.) Hubb.	C4	Herbarium specimen no. 7839	Me
	Panicum anabaptistum Steud.	C4	Herbarium specimen no. 6039	He
	Panicum fluviicola Steud.	C4	Herbarium specimen no. 8261	He
	Panicum laetum Kunth	C4	Herbarium specimen no. 6911	Xe
	Panicum subalbidum Kunth	C4	Herbarium specimen no. 5811	He
	Panicum turgidum Forssk.	C4	Herbarium specimen no. 7250	Xe
	Pennisetum pedicellatum Trin.	C4	Herbarium specimen no. 6533	Me
	Schizachyrium exile[a] *(Hochst.) Pilger*	C4	Herbarium specimen no. 10747	Xe
	Setaria sphacelata (Schumach.) Moss	C4	Herbarium specimen no. 5802	He
	Vetiveria nigritana (Benth.) Stapf	C4	Herbarium specimen no. 40837	Hy/He
	Vossia cuspidata (Roxb.) Grill.	C4	Herbarium specimen no. 8354	Hy
Typhaceae	*Typha domingensis*[a] *Schum. & Thonn*	C3	Herbarium specimen no. 13089	Hy

[a] Found totally sterile.
[b] Replaces *Brachiaria jubata*.

The two other thirds include mesophytes, that avoid extremes of moisture and drought, and xerophytes, which normally subsist with relatively little moisture (Watson and Dallwitz, 1992 onwards; Poilecot, 1999; César and Lebrun, 2003). In our dataset, several hydrophytes and helophytes among the Cyperaceae and the Poaceae exhibit a C_4 photosynthetic pathway (Watson and Dallwitz, 1992 onwards; Schwartz and Mariotti, 1996) (Table 2). In this study, we consider the Poaceae systematic (subfamilies) based on the molecular phylogenetic analysis by the Grass Phylogeny Working Group (Kellogg, 2001). The modern soil and plant phytolith collection is curated at CEREGE (Aix en Provence, France).

Phytolith extraction from soil and mud samples was done using approximately 10 g of material. Chemical treatment included carbonate dissolution with hydrochloric acid (HCl, 37% overnight), organic matter (OM) oxidation with hydrogen peroxide (H_2O_2 at 33%, at 90 °C), iron removal (with $C_6H_5Na_3O_7$ and $Na_2O_4S_2$, H_2O_2), and clay removal by decantation. Finally, densimetric separation with zinc bromide heavy liquid ($ZnBr_2$) set at d = 2.3 was used to concentrate the silica particles (including phytoliths, diatoms, sponge spicules, etc.). To extract phytoliths from the botanical specimens, we used up to 5 g of thoroughly washed plant material for the species sampled in the field, but less than 1 g for those sampled in the herbarium. For this study, only leaves were considered. OM was digested by successive nitric/perchloric acid treatments (HNO_3/$HClO_4$) at 80–90 °C, and completed by digestion with hydrogen peroxide (H_2O_2). We used glycerine as mounting medium to allow the observation of phytoliths in the three dimensions and counting. However, to get good quality photographs of the phytoliths we mounted extra slides with Canada Balsam. Microscopic observations were done at × 400 magnification. We counted a minimum of 400 phytoliths for the soil/mud samples. For some samples, counting was carried out until material was exhausted (Appendix 1). Diatoms and sponge spicules were observed in all sediment samples but not counted. We counted a minimum of 200 phytoliths (including short and long cells) for each plant. However, four specimens were found sterile: *Cyperus papyrus*, *Digitaria ciliaris*, *Schizachyrium exile*, and *Typha domingensis*.

Phytoliths were described and classified according to their 3D morphology, and following the international code of phytolith nomenclature (Madella et al., 2005) (Table 3). We observed and counted separately 38 types of grass silica short cells (GSSCs) (Plate I),

Table 3
Phytolith morphotypes observed in soils (S), Poaceae (POAC) and Cyperaceae (CYPE) specimens from Chad.

Phytolith categories/types and descriptions		Observed in
Grass silica short cells (Poaceae)		
Rondels (conical/cylindrical bodies, with round/oval base, size: Ø 8–12 μm (except Ro-8) and h = 5–12 μm (except Ro-7))		
Ro-1	Conical, top truncated, top and base oval	(S), (POAC)
Ro-2	Conical, top keeled/spiked	(S), (POAC)
Ro-3	Conical, top tapering	(S), (POAC)
Ro-4	Cylindric, constricted sides	(S), (POAC)
Ro-5	Cylindric, base and top reniform	(S), (POAC)
Ro-6	Cylindric, base oval, slightly constricted	(S), (POAC)
Ro-7	Cylindric, base/top round/squared with +/− regular outlines ("chimney" or "volcano" bodies), h = 16–20 μm	(S), (POAC)
Ro-8	Oblong, to keeled/truncated, L ≥ 15 μm	(S)
Trapeziform bodies (six-sided), size: L = 8–10 μm		
Tra-1	Cubic/parallelepipedal bodies	(S), (POAC)
Bilobates (bodies with two lobes connected by a +/− long shank), size: L = 10–25 μm: "short" or L > 25 μm: "long", h ≤ 5 μm: "tabular" or h > 5 μm: "trapeziform/parallelepipedal"		
Bi-1	Short, tabular, truncated lobes	(S), (POAC)
Bi-2	Short, tabular, round lobes	(S), (POAC)
Bi-3	Long, tabular, truncated lobes	(S), (POAC)
Bi-4	Long, tabular, round lobes	(S), (POAC)
Bi-5	Long, tabular, concave lobes	(S), (POAC)
Bi-6	Long, tabular, notched lobes	(S), (POAC)
Bi-7	Short, tabular, concave lobes	(S), (POAC)
Bi-8	Short, tabular, notched lobes	(S), (POAC)
Bi-9	Short, tabular, almost equidimensional, round/truncated lobes, missing shank	(S), (POAC)
Bi-10	Parallelepipedal, truncated lobes	(S), (POAC)
Bi-11	Short trapeziform, base bilobate, variable top, L > h	(S), (POAC)
Bi-12	Short trapeziform, base constricted in the middle, top squared to vaguely bilobate and slightly concave in side view, bodies with very high trapezoid section, L ≤ h	(S), (POAC)
Bi-13	Trapeziform, base bilobate with one supplementary lobe, variable top, L > h	(S), (POAC)
Bi-14	Trapeziform, base bilobate with +/− concave lobes, variable top, L > h	(S), (POAC)
Bi-15	Tabular to parallelepipedal, truncated to round lobes, very long shank (L of shank > L of one lobe) with remarkable swelling	(S), (POAC)
Crosses (equidimensional bodies, 4- or 3-lobed), size: L = 8–12 μm, h ≤ 5 μm: "tabular" or h > 5 μm: "trapeziform"		
Cr-1	Tabular, 3-lobed	(S), (POAC)
Cr-2	Tabular, 4-lobed rounded	(S), (POAC)
Cr-3	Tabular, 4-lobed truncated/angular	(S), (POAC)
Cr-4	Trapeziform, 3-lobed	(S), (POAC)
Cr-5	Trapeziform, 4-lobed, cross top	(S), (POAC)
Cr-6	Trapeziform, 4-lobed, polyhedral/keeled top, L > h	(S), (POAC)
Cr-7	Trapeziform, 4-lobed, polyhedral/keeled top ("Eiffel tower"), L ≤ h	(S), (POAC)
Cr-8	Tabular to parallelepipedal, 4-lobed, loss of axial symmetry, equal opposed lobes	(S), (POAC)
Polylobates (modified bilobates with one to several supplementary lobes on the shank), size: 18–25 μm		
Poly-1	Tabular, 3 to 4 round well-defined lobes	(S), (POAC)
Saddles (bodies with two opposite convex edges and two opposite concave edges in top view, "battles axes with double edges"), size: L = 8–12 μm, h ≤ 5 μm: "tabular" or h > 5 μm: "trapeziform"		
S-1	Tabular, equidimensional convex and concave edges	(S), (POAC)
S-2	Tabular short, convex edges shorter than concave edges	(S), (POAC)
S-3	Tabular long, convex edges longer than concave edges	(S), (POAC)
S-4	Trapeziform equidimensional to long, base oblong, round or vaguely constricted, saddle top, "saddle-rondel" (Strömberg, 2003)	(S), (POAC)
S-5	Trapeziform, base bilobate, top saddle-shaped, "saddle-bilobate" (Strömberg, 2003)	(S), (POAC)
Other phytolith types (non-GSSCs)		
Acicular bodies		
Aci-1	Smooth (50–75 μm)	(S), (POAC), (CYPE)
Aci-2	Smooth, often infilled with black material (40–50 μm)	(S), (POAC)
Aci-3[a]	Smooth, compartimented ("multi-layered trichome" Strömberg, 2003) (30–100 μm)	(S)
Blocky bodies		
Blo-1	Long acicular to oblong, sometimes pinched-point, often infilled with black material (50–75 μm)	(S), (CYPE)
Blo-2	Irregular with non well-defined shape (30–100 μm)	(S), (CYPE)
Blo-3	Parallelepipedal to cubic, granulate (25–100 μm)	(S)
Blo-4	Perfectly cuneiform (bulliform cell) (30–100 μm)	(S), (POAC)
Blo-5	Parallelepipedal with constricted sides, approximately cuneiform (30–100 μm)	(S), (POAC), (CYPE)
Blo-6	Cubic, smooth, often infilled with black material (25–75 μm)	(S)
Blo-7	Parallelepipedal, smooth, often infilled with black material (25–100 μm)	(S), (CYPE)
Blo-8	Parallelepipedal, smooth, crenate margins, often infilled with black material (40–100 μm)	(S), (POAC), (CYPE)
Blo-9	Orbicular to ovate, smooth, slightly curved (10–15 μm)	(S), (CYPE)
Blo-10	Angular, attenuate ends ("sclereid", Neumann et al., 2009; Strömberg, 2003) (45–50 μm)	(S)
Blo-11[a]	Trapeziform (h = 15 μm), smooth, long and hexagonal top/base (37 μm)	(CYPE)
Elongate bodies		
El-1[a]	Cylindric, smooth (100–150 μm)	(S)
El-2	Tabular/parallelepipedal bodies, pinched-point (50–75 μm)	(S)
El-3	Tabular/parallelepipedal bodies with smooth, sinuate or echinate margins (50–200 μm)	(S), (POAC), (CYPE)
El-4	Cylindric, laminate, with a median swelling (75–150 μm)	(S)
El-5[a]	Unciform, smooth ("simple solid trichome", Strömberg, 2003)	(S), (POAC)
El-6	Reflexed parallelepipedal, smooth (30–75 μm)	(S), (CYPE)

(continued on next page)

Table 3 (*continued*)

Phytolith categories/types and descriptions		Observed in
Epidermal silicified structures		
Str-1[a]	Articulated epidermal structure of Cyperaceae-papillae (more than three articulated elements) (100–200 μm)	(S)
Str-2[a]	Articulated epidermal structure of GSSCs (more than three articulated elements) (100–200 μm)	(S)
Sto-1	Silicified stomate (25–50 μm)	(S), (POAC), (CYPE)
Trac-1	Silicified tracheid (50–150 μm)	(S), (POAC), (CYPE)
Globular bodies		
Glo-1	Echinate (Ø 8–17 μm)	(S)
Glo-2	Granulate (Ø 12–17 μm)	(S)
Glo-3	Granulate/tuberculate with small smooth rounded projections and often dark core (Ø 8–15 μm)	(S)
Glo-4	Granulate/tuberculate with a central vacuum (Ø 8–15 μm)	(S)
Glo-5	Psilate (Ø 15–20 μm)	(S), (POAC), (CYPE)
Glo-6	Micro-echinate (Ø 15–20 μm)	(S)
Glo-7	Tuberculate with large smooth rounded projections (Ø 15–20 μm)	(S)
Glo-8	Psilate to sinuate, large and often infilled (30–40 μm)	(S)
Polyhedral bodies		
Pol-1	"Subcylindric, distinctly anisopolar, upper part polygonal prismatic with conical top" (from Eichhorn et al., 2010) (20–30 μm)	(S)
Polyhedral plates		
Pla-1	Irregular articulated pieces, rugulate ("jigsaw", Strömberg, 2003) (50–75 μm for each piece)	(S)
Pla-2[a]	Rectangular, lacunate (30–40 μm)	(S)
Pla-3[a]	Stellate, psilate (25–30 μm)	(S), (CYPE)
Pla-4	Planar, hexagonal, scorbiculate, cavate in the center (30–35 μm)	(S), (CYPE)
Pla-5	"Sinuous shape, knobby apex, psilate sculpturing, satellites absent = NKXWI" (from Ollendorf, 1992) (15–20 μm)	(S), (CYPE)
Pla-6	"Angular to sub-rounded shape, pointed apex, psilate sculpturing, satellites present = A(R)KXWI" (from Ollendorf, 1992); papillae cell or "hat-shaped" (Piperno, 1988) (10–20 μm)	(S), (CYPE)
Pla-7[a]	"Rounded shape, knobby apex, psilate sculpturing, satellites absent = RPXWI" (from Ollendorf, 1992); papillae cell or "hat-shaped" (Piperno, 1988) (10–15 μm)	(S), (CYPE)
Pla-8[a]	Orbicular, stellate inside (hair base) (Ø 40–60 μm)	(S)
Pla-9[a]	Segmented, psilate ("vertebral column", Strömberg, 2003) (25–40 μm)	(S), (POAC)
Undefined		
Undescriptible phytolith elements, broken or without distinguishable shapes		(S)

[a] Not in Plate II.

and 42 non-grass silica short cells (non-GSSCs) (Plate II). Among the GSSCs, we distinguished rondel phytolith types according to their overall shape (circular, cylindric, oblong), and the shape of their top (keeled, tapering or truncated) (Ro-1 to -8). We found only one type of trapeziform short-cell in the Chad samples (Tra-1). More diversity was observed within the bilobate short cells category, for which we observed and counted separately 15 different types (Bi-1 to -15). Bilobate types were distinguished according their transversal section (tabular, trapeziform, parallelepipedal), the shape of the lobes (truncated, round, concave, notched), and their length. We distinguished cross phytolith types according to their transversal section (tabular, trapeziform), the number of lobes, and the shape of the top (Cr-1 to Cr-8). We observed one type of polylobate (tabular) with three or four lobes (Poly-1). Saddle-shaped phytoliths were distinguished according to their transversal section (tabular, trapeziform), the shape of the base, and the length of the convex edges (S-1 to -5). Among the 42 different types that are non-grass silica short cells (non-GSSCs) (Table 3, Plate II), we distinguished blocky bodies according to their 3-D structure (oblong, cubic, parallelepipedal, cuneiform, orbicular, angular), and their ornamentations (smooth, granulate). Elongate bodies were distinguished according to their transversal section (tabular to parallelepipedal, cylindric, unciform), and particularities (pinched-point, reflexed, swelling). Globular phytoliths were distinguished according to their ornamentation (e.g. granulate, echinate). Polyhedral bodies (size<40 μm) include the subcylindric, distinctly anisopolar body with the upper part polygonal prismatic and conical top observed in Commelinaceae species (Eichhorn et al., 2010). Polyhedral plates include the Papillae "hat-shaped" phytoliths observed in Cyperaceae (Ollendorf et al., 1987, 1988; Piperno, 1988; Ollendorf, 1992), and other planar bodies of different shapes (e. g. orbicular, segmented). Finally, we also observed silicified stomata, tracheid bodies, and articulated epidermal silicified structures.

We analyzed the relative abundance of each phytolith type in the Cyperaceae and Poaceae botanical specimens. For the Poaceae, for which the phytolith diversity is the highest, we ran a value-test analysis (VT) (Lebart et al., 2000) to identify the GSSCs that are statistically the most characteristic for a certain ecological group of grass species. The VT is a criterion used for characterizing a group of observations (here grass species) according to a continuous or categorical variable (here the aquatic, mesophytic, and xerophytic ecological categories). The groups are defined by categories from a discrete variable (GSSC types). The VT analysis compares the values of a descriptive statistic indicator computed on the whole sample, and then computed on a subsample related to the group. The value test is calculated as follows,

$$ValueTest = \frac{\mu_g - \mu}{\sqrt{\frac{n-n_g}{n-1} \times \frac{\sigma^2}{n_g}}}$$

where μ_g is the mean of the group, μ the mean of the whole dataset, n the size of the group, n_g the size of the whole dataset, and σ^2 the variance (Lebart et al., 2000). We considered that a GSSC type was characteristic of a group of grasses (aquatic, mesophytic, or xerophytic) if the association phytolith-group was exclusive and supported by a significant positive test-value, and if the mean abundance of the phytolith type on the ecological group was > 2% (Appendix 2). We then looked at the abundance of these characteristic cohorts of GSSC types in the soil and mud samples.

We also calculated phytolith ratios such as the D/P ratio of decorated globular phytoliths over GSSCs, which is a measure of the abundance of ligneous indicators versus grasses (Bremond et al., 2008b). The aridity index Iph is the ratio of saddle GSSCs over saddle, bilobate and cross GSSCs (Diester-Haass et al., 1973). It may be used to measure the abundance of C_4 short-grasses (mostly Chloridoideae) over C_4 tall-grasses (mostly Panicoideae) (Bremond et al., 2004). The Fs index is the percentage of silicified bulliform cells over the total phytolith sum that may be used to evaluate grass-water stress (Bremond et al., 2004). The non-parametric test of Mann–Whitney (MW test) was used to detect significant differences in the index mean values between vegetation zones (Sudanian, Sahelian, and Lake Chad).

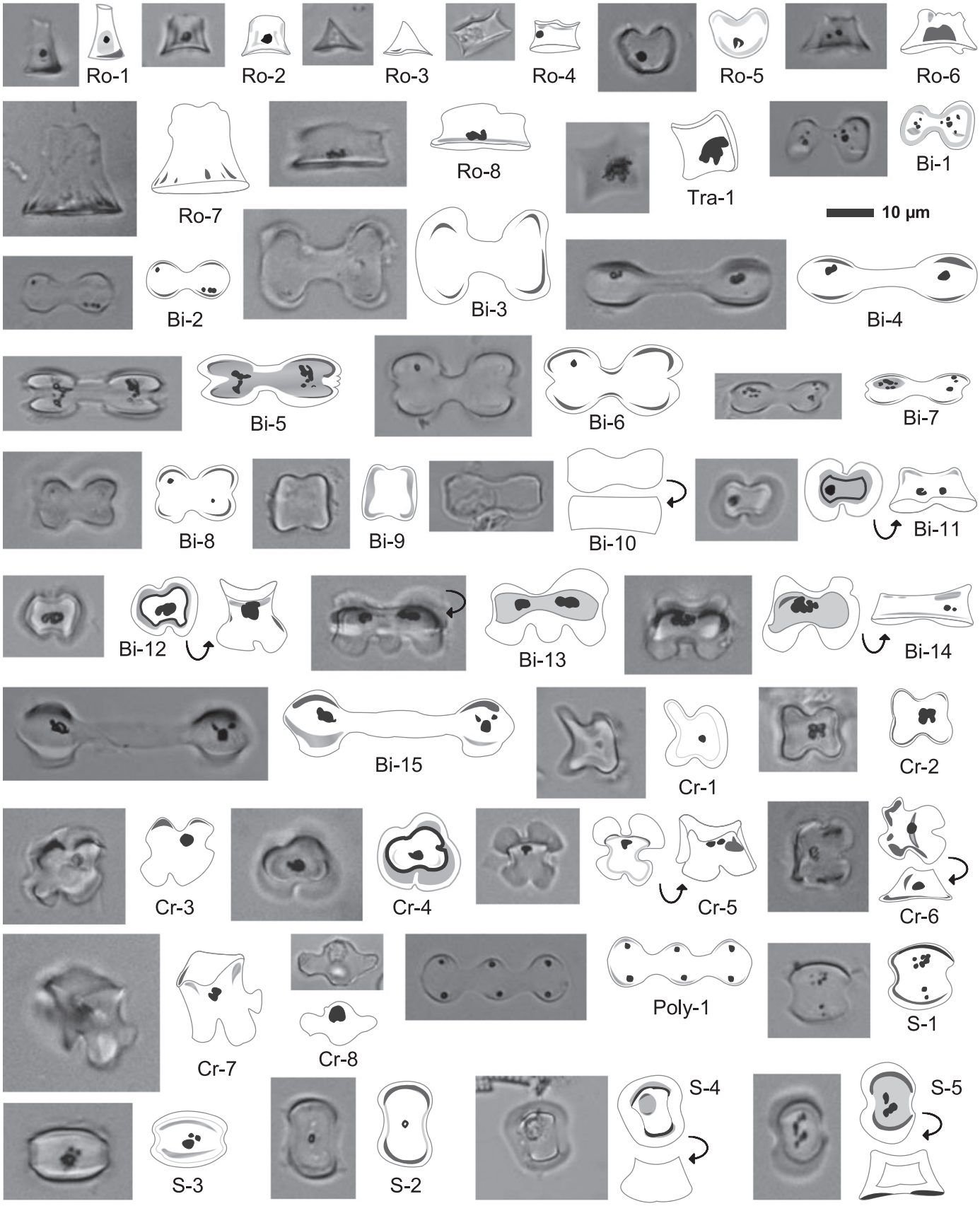

Plate I. Grass silica short cells. Micrographs and drawings of the grass silica short cell types (GSSCs) observed in soils and plant specimens from Chad. See Table 3 for detailed descriptions of the phytolith morphologies. Ro: rondels; Bi: bilobate; Cr: cross; Poly: polylobate; S: saddles.

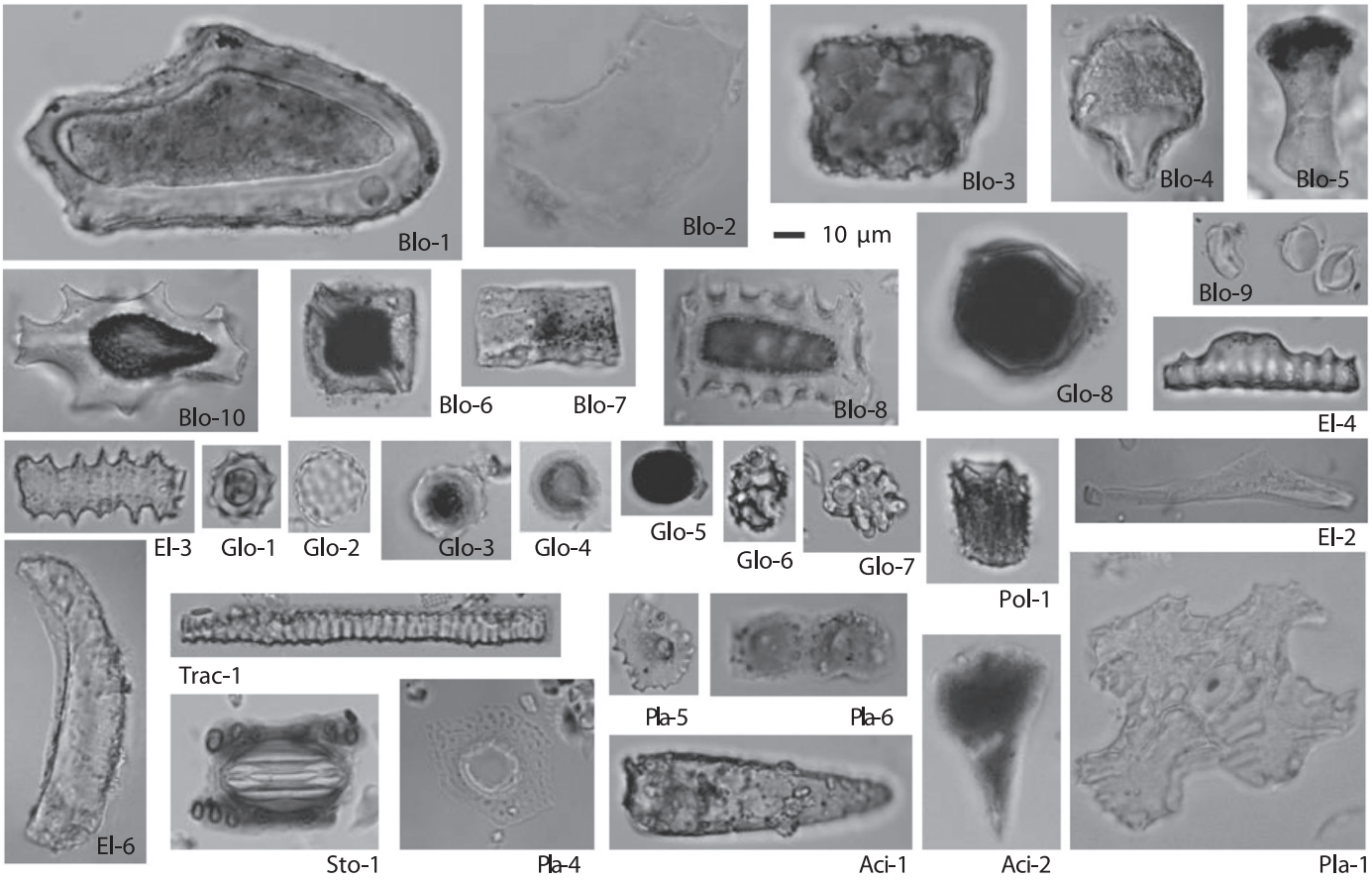

Plate II. Non-grass silica bodies. Micrographs of phytolith types (other than grass silica short cells) observed in soils and plant specimens from Chad. Blo: blocky bodies; El: elongates; Glo: globular bodies; Pol: polyhedral bodies; Pla: polyhedral plates; Sto: stomata; Trach: tracheid; Aci: acicular bodies.

4. Results

4.1. Phytoliths in the botanical specimens

In the Cyperaceae species, the most represented phytolith types are the elongate tabular with smooth/sinuate edges (El-3), found in 6 over 7 species, and accounting for up to 37% in some species but absent in *Cyperus difformis*, and the Papillae "hat-shaped" tabular bodies with pointed apex (Pla-6), found in 5 over 7 species, and accounting for 50% to 98% of the total phytolith sum in most species, except *Cyperus articulatus* and *Cyperus alocuperoides* (Fig. 2). *Schoenoplectus roylei* exhibits the greatest diversity of silicified Papillae with three

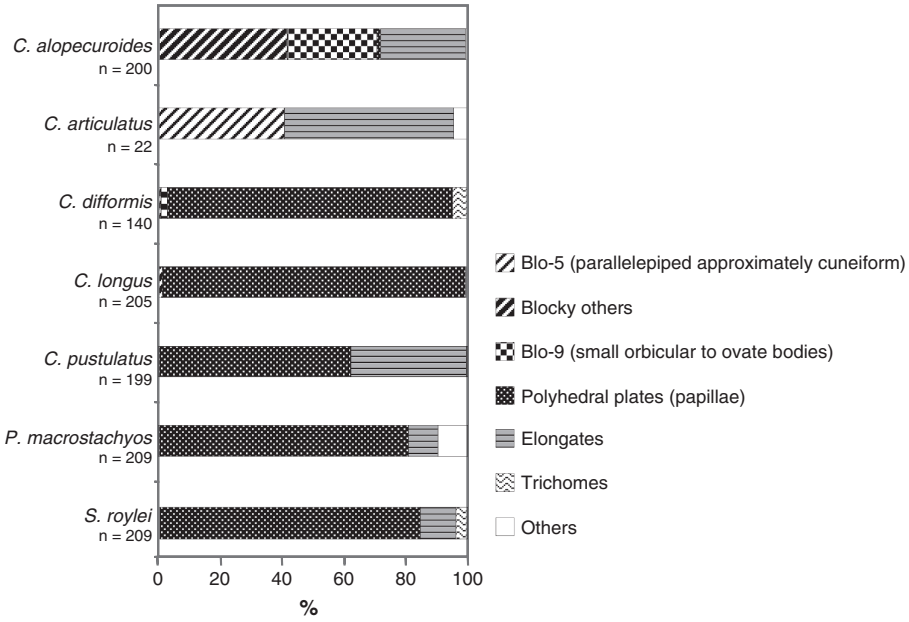

Fig. 2. Relative abundance of phytolith types observed in Cyperaceae.

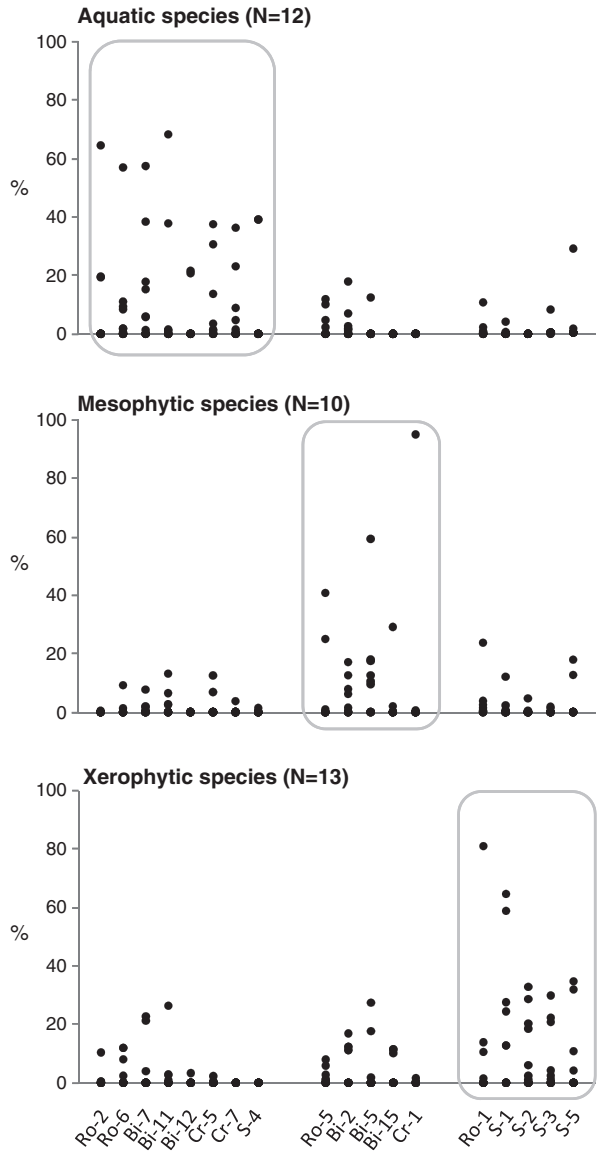

Fig. 3. Cohort of phytolith types (%) identified by the value-test analysis for the aquatic, mesophytic, and xerophytic grass species.

different types present in its leaves (Pla-4, -5, -6 and -7). *Schoenoplectus roylei* also produces globular smooth phytoliths, such as *Pycreus macrostachyos* (Appendix 1). *Cyperus alocuperoides* is the specimen that exhibits the most remarkable phytolith assemblage, with only 27% elongate phytoliths, but 29% blocky bodies with crenate margins (Blo-8), and almost 30% of orbicular smooth bodies (Blo-9), one of the new phytolith types to be attributed to Cyperaceae (Plate II). Four additional phytolith types are also new for Cyperaceae: the large (50–75 μm) acicular to ovoid blocky body (Blo-1), which is often infilled with black material, the reflexed parallelepipedal elongate (El-6), the vaguely cuneiform body (Blo-5) (Plate II), and the polyhedral trapeziform smooth body (Blo-11) (Table 3); Blo-11, however, was only observed once.

In the Poaceae species, silicified short cells (GSSCs) represent 56% to 100% of the silica bodies included in the leaves (Appendix 1). In our dataset, *Echinochloa pyramidalis*, *Pennisetum pedicellatum*, and *Panicum fluviicola* exhibits the highest percentage of long cell phytoliths (acicular and blocky bodies, plus elongates) (25% to 39%). Among the GSSCs, rondels, which occur in 23 out of 35 species, were found most abundant in the Chloridoideae *Eragrostis tremula* (95%), *Eragrostis squamata* (82%), and *Sporobolus cordofanus* (74%), and in the Ehrhartoideae *Leersia hexandra* (78%); all other grass species had <32% of rondel phytoliths in their epidermis. The most common rondel types are the truncated Ro-1, crescent Ro-5, and truncated with a slightly constricted base Ro-6. The keeled type Ro-2, which occurs in seven grass species, was found most abundant in *L. hexandra* (64%). All rondel phytolith types are ≤12 μm high, except type Ro-7 (Plate I, Table 3) which was observed only in very low amounts in *P. fluviicola* (Panicoideae) (5% of the GSSC) and *E. tremula* (0.5%). Bilobates, which occur in 30 out of 35 species, were observed in Panicoideae (21/21 sp.), Chloridoideae (5/9 sp.), Aristidoideae (2/2 sp.) and Ehrhartoideae (2/2 sp.). They account for more than 95% of the GSSCs in some Aristidoideae, Panicoideae and Chloridoideae (e.g. *Aristida mutabilis*, *Hyparrhenia barteri*, *Ctenium elegans*). Tabular bilobates with notched, concave, and truncated ends (Bi-8, Bi-7, and Bi-2) are the most common; they occur in 27 over 35 species and may account for more than 50% of the GSSCs in *Oryza longistaminata*, *Acroceras amplectens*, and *E. pyramidalis*. We observed and counted separately several tall trapezifom bilobate types (Bi-11 to -14, height > 5–10 μm), which are variants of the *Stipa*-type (Fredlund and Tieszen, 1994). Trapeziform bilobates only occur in some Panicoideae species and in the Aristidoideae *Aristida stipoides*. The greatest percentages of trapeziform bilobates were observed in *Vossia cuspidata*. Two species, *V. cuspidata* and *Vetiveria nigritana* exclusively produce trapeziform bilobates. Long bilobates (length 26–40 μm, types Bi-3 to -6, and Bi-15) were observed in Panicoideae (10/21 sp), Aristidoideae (2/2 sp), and Chloridoideae (2/9 sp). They account for up to 95% in the Chloridoideae *C. elegans*. Cross phytoliths, which occur in 23 out of 35 species were observed in Panicoideae (20/21 sp.), Ehrhartoideae (2/2 sp.), and Chloridoideae (only *S. cordofanus*). Cross phytoliths are abundant in the Panicoideae *Loudetia simplex* (96%), *V. nigritana* (62%), and *Panicum subalbidum* (58%). The most common cross types are the tabular type Cr-2 and the trapeziform types Cr-5 to -7. Only trapeziform crosses are found in some Panicoideae such as e.g. *V. nigritana*, *E. pyramidalis*, and *Panicum turgidum*. Saddle phytoliths, which occur in 18 out of 35 species, were observed in every Chloridoideae species (8/9 sp.), in some Panicoideae (8/21 sp.) and in the Arundinoideae *Phragmites australis*. Saddle phytoliths may account for up to 100% of the GSSC in some Chloridoideae species such as in *Chloris pilosa*, *Dactyloctenium aegyptium*, and *Schoenefeldia gracilis*, and up to 68% in *P. australis*. In *P. australis*, however, we only observed the trapeziform saddles S-4 and S-5 (Plate I, Appendix 1). S-4 may also be called "saddle-topped short trapezoid" (Ollendorf et al., 1988), "plateaued-saddle" (Piperno and Pearsall, 1998) or "saddle-rondel" (Strömberg, 2003), whereas S-5 is equivalent to "saddle-dumbbell" (Strömberg, 2003).

In the Poaceae, silicified long cells (non-GSSCs) such as the tabular elongate bodies (El-3) and acicular hair cells (Aci-1 and -3) were found in most species (up to 31% in *Pennisetum pedicellatum*). Silicified bulliform cells (types Blo-4 and Blo-5) were found in 19/35 species, in low percentages (<14%). The parallelepipedal blocky type with crenate margins Blo-9, which we observed in Cyperaceae, was also observed in nine Poaceae species at <8%. Other non-GSSC types, such as a globular smooth phytolith (Glo-5), stomata (Sto-1), and tracheid silicified elements (Trac-1) were also observed, but in very low proportions (<3%) (Appendix 1).

4.2. Phytolith cohorts for aquatic, mesophytic, and xerophytic grasses

The VT analysis performed on our plant dataset has identified 18 types of GSSCs (out of 38) that preferentially occur in aquatic, mesophytic, and xerophytic Poaceae species (Appendix 2, Fig. 3). It is the cohort of phytolith types (rather than individual types) that is identified as characteristic for the habitat-specific grasses included in our dataset. The cohort of GSSCs associated to the aquatic grasses includes rondel phytoliths (Ro-2, Ro-6), a tabular bilobate with concave ends

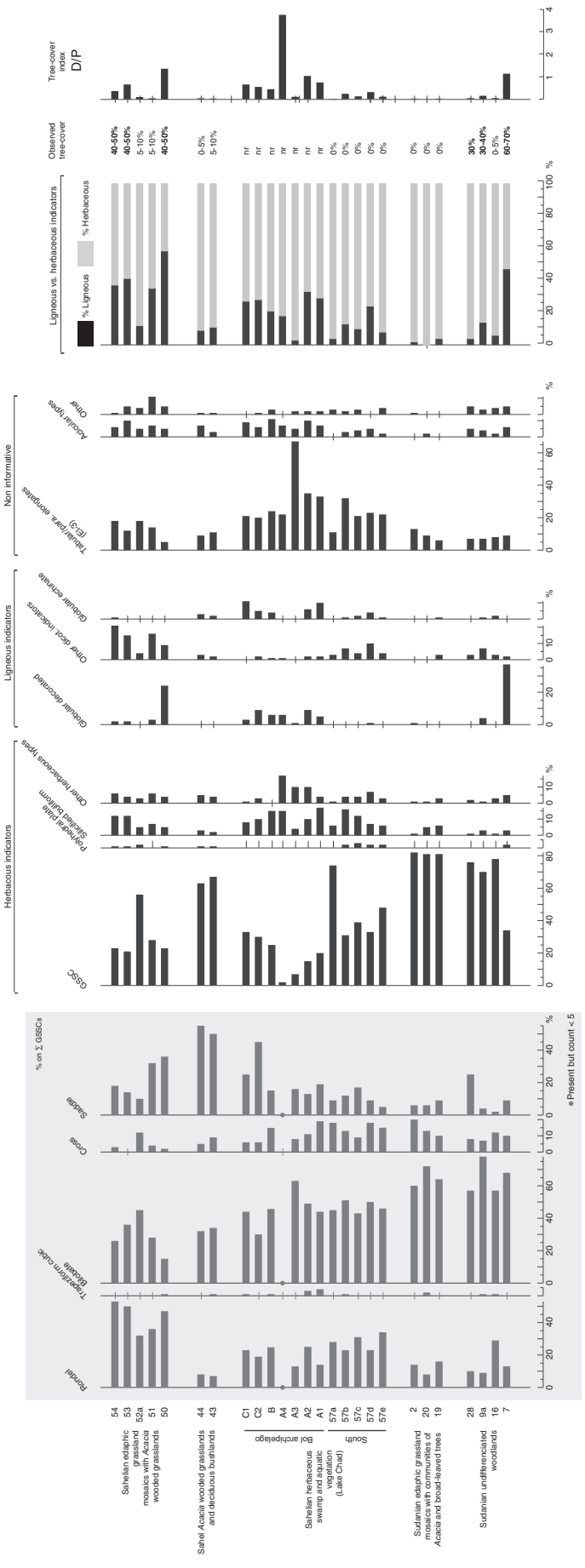

Fig. 4. Phytolith percent diagram of mud/surface soil samples from Chad.

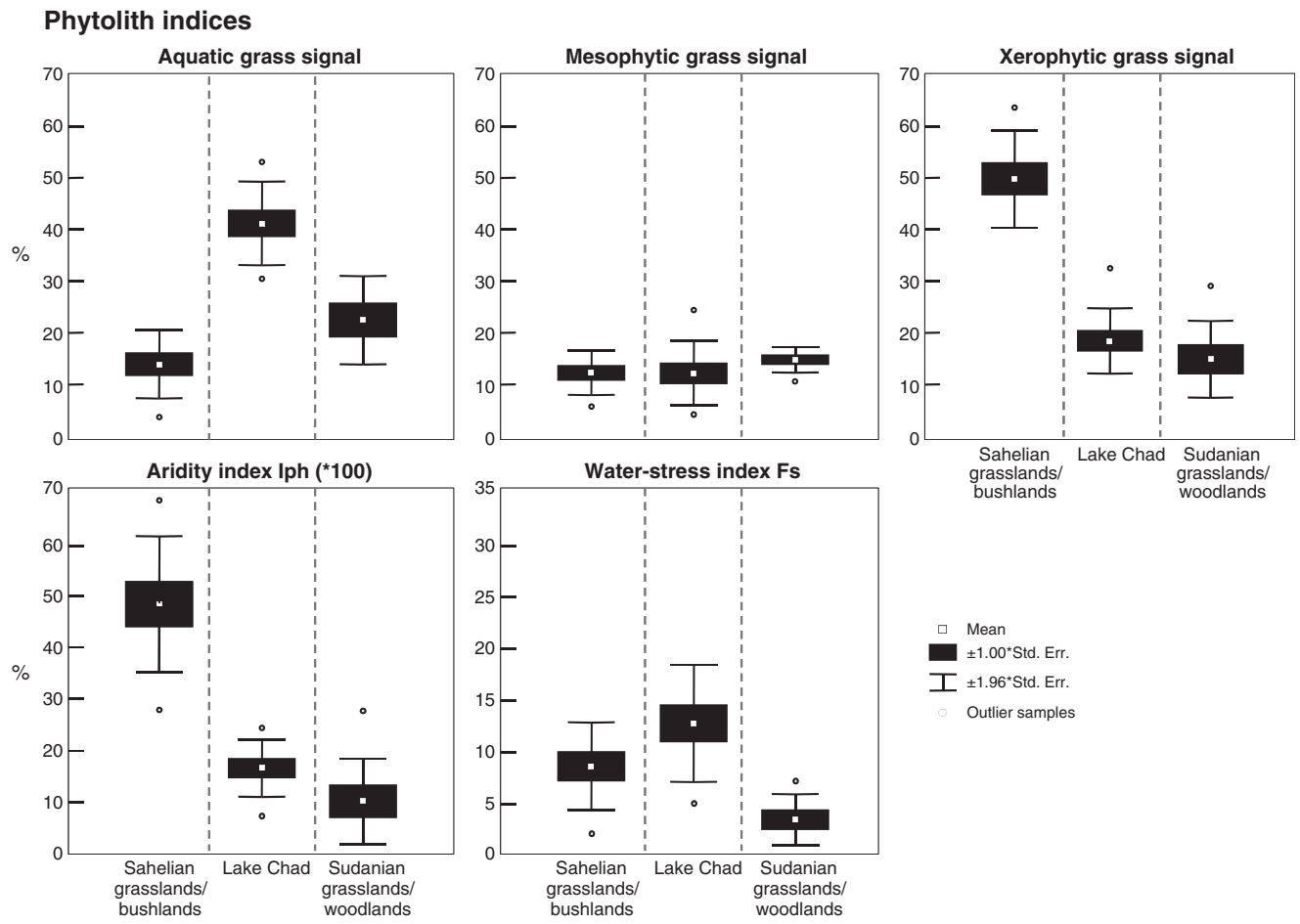

Fig. 5. Comparison between the "aquatic", "mesophytic", and "xerophytic" grass signals (%), aridity index (Iph, %) and water stress index (Fs, %) calculated for the mud/surface soil samples from the Sahelian and Sudanian Chadian regions, as well as from Lake Chad. Descriptive statistics as mean values for phytolith indices, standard error of the mean (SE), and 95% confidence interval (1.96 ± SE) are given.

(Bi-7), trapeziform bilobates (Bi-11, Bi-12), trapeziform crosses (Cr-5, Cr-7), and a trapeziform saddle (S-4). A cohort of five GSSCs was identified as characteristic for mesophytic grasses. It includes the crescent rondel (Ro-5), a short tabular bilobate (Bi-2), long tabular bilobates (Bi-5, Bi-15), and the tabular 3-lobed cross (Cr-1). The cohort of GSSCs associated to the xerophytic grasses includes a rondel type (Ro-1), the tabular saddles (S-1, -2, and -3), and a trapeziform saddle (S-5).

4.3. Taxonomic attributions of the phytolith types in the surface soils and mud samples

We made taxonomical attributions of the phytoliths observed in the soil and mud samples based on observations of our own plant material (Table 2) and the literature. In these surface samples we observed 80 different phytolith types, among which 57 are attributed to herbaceous taxa, 10 to ligneous plants (including palms), and 13 others that we believe are non informative (Fig. 4, Appendix 1). The herbaceous indicator category includes isolated GSSCs plus articulated epidermal structure (Str-2) strictly produced by Poaceae (Twiss et al., 1969; Mulholland, 1989; Mulholland and Rapp, 1992), as well as different blocky types including the silicified cuneiform (Blo-4) and parallelepiped (Blo-5) bulliform cells (Twiss et al., 1969; Kondo et al., 1994). The herbaceous category also includes various blocky (Blo-1, -8, -9 and -11), and elongate (El-6) that we observed in some Poaceae and Cyperaceae species (Appendix 1), the isolated and articulated silicified Papillae from Cyperaceae (Pla-4, -5, -6, -7, Str-1), a Commelinaceae-type phytolith (Pol-1) (Eichhorn et al., 2010), a globular body type (Glo-6) associated to Marantaceae/Costaceae (Runge, 1999; Strömberg, 2003), and other silica bodies previously described in herbaceous species (El-4, Pla-2, -3, -9) (Runge, 1999; Ball, 2002; Strömberg, 2003; Thorn, 2004; Mercader et al., 2009). The ligneous indicator category includes six decorated globular types (Glo-1, -2, -3, -4, -7, -8) (Scurfield et al., 1974; Piperno, 1988; Kondo et al., 1994; Mercader et al., 2009; Neumann et al., 2009) and some blocky and elongate bodies (Blo-3, -10, El-1, -2) (Runge, 1999; Strömberg, 2003; Mercader et al., 2009). The non-informative category includes silica bodies with various morphologies such as elongates (El-3) (Ball, 2002; Strömberg, 2003; Wallis, 2003), acicular hair cells (Aci-1, -2, -3) (Palmer et al., 1985; Piperno, 1988; Strömberg, 2003; Mercader et al., 2009), globular smooth phytoliths (Glo-5) (Ellis, 1979; Piperno, 1988; Kondo et al., 1994; Strömberg, 2003; Mercader et al., 2009), and other types with uncertain or imprecise assignation (Blo-2, Blo-6, Blo-7, El-5, Sto-1, Trac-1, Pla-1, Pla-8) (Strömberg, 2003; Mercader et al., 2009).

4.4. The phytolith signal of vegetation in the surface soils and mud samples

The general physiognomy of the grass-dominated vegetation we sampled in Chad is well reproduced by the relative abundance of herbaceous and ligneous indicator phytoliths in the soils. Indeed, the abundance of ligneous indicator phytoliths rarely exceeds 30% in the 26 surface soil samples, and D/P values are generally <1 in agreement with the scarcity of trees and shrubs observed at the sampling sites

(Fig. 4). In four samples (50, 7, A2, A4), however, the decorated globular phytoliths (associated to ligneous dicots) account for more than 10% and D/P is >1. In samples 50 and 7, the high D/P values (D/P>1) and relatively high percentages of ligneous indicators (46–57%) are in agreement with the locally dense observed tree cover, which was of 40–50% at the sampling site 50 (a closed-*Acacia* temporary swamp in the Sahelian zone), and of 60–70% at the sampling site 7 (a dense woodland from the Sudanian zone). In sample A4 from the Lake Chad Bol archipelago, the unrealistically high D/P index of 3.75 is most likely biased by the little number of GSSCs and globular phytoliths (20 in total) that could be counted in this sediment rich in non-informative, mainly elongate phytoliths (Appendix 1).

Differences in the grass composition of the vegetation that exists between the arid Sahelian zone (>13°N) and the humid Sudanian zone (<10°N) is expressed by differences in the phytolith assemblages, notably by the GSSCs. Values of phytolith indices Iph and Fs increase along the S–N latitudinal gradient of increasing aridity (Fig. 4). Mean Fs index, which is of 3% for the Sudanian zone, is of 7% for the Sahelian samples. Mean Iph index, which is of 10% for the Sudanian zone, is up to 49% for the Sahelian zone (Fig. 5). These differences between the Sudanian and Sahelian regions (Lake excluded) are significant (test Mann–Whitney, $p<0.05$).

The swamp and aquatic vegetations sampled in Chad also exhibit different phytolith signals than the vegetations sampled on well-drained soils. The most obvious difference is made by the cohort of GSSCs characteristic for aquatic grasses (Fig. 5), which is significantly more abundant (42% in average) in the Lake Chad samples, than in the Sudanian (ca 23%) and in the Sahelian (ca 14%) samples (test Mann–Whitney, $p<0.05$), in agreement with the abundance of helo- and hydrophytic grasses at this permanent water-body. Papillae-cells produced by sedges are poorly represented in the soils, where they account for <3% even in the Cyperaceae rich-environments of Lake Chad and of other swampy areas in the Sahelian zone (Fig. 4). The mud samples from these Cyperaceae-rich environments were found rich in elongate phytoliths (10–69%) and in silicified bulliform cells (4–16%) (Fig. 4), and relatively poor in GSSCs (2–48%, sample 57a excluded) compared to the samples from the well-drained soils that we sampled in the Sudanian and Sahelian zones (>30% to 78%).

The cohorts of GSSCs that we identified using the value-test analysis help to discriminate the aquatic vegetation from the non-aquatic vegetation, and improve the discrimination between the xerophytic-rich Sahelian grasslands and the Sudanian vegetation mosaics and woodlands. Indeed, the abundance of the cohort of phytoliths for xerophytic grasses averages 50% in Sahelian samples, whereas it does not exceed 19% on average in Sudanian and aquatic samples. The cohort identified as characteristic of mesophytic grasses, however, brings little discrimination between the Sudanian, Sahelian, and aquatic zones (Fig. 5). Indeed, the abundance of the cohort of phytoliths for mesophytic grasses averages 15% in all three vegetation zones.

5. Discussion

Our study provides new quantitative phytolith data for seven Cyperaceae species, which confirm the general pattern of phytolith production. We found that most Cyperaceae (5/7 species) produce "hat-shaped" Papillae phytoliths in abundance (Fig. 2), in agreement with previous studies (Ollendorf et al., 1987; Ollendorf, 1992; Bamford et al., 2006). Two species, *Cyperus alopecuroides* and *Cyperus articulatus*, however, mainly produce blocky and elongate silica bodies (Fig. 2). Among the blocky and elongate phytolith types that we observed in the Cyperaceae, only the orbicular smooth Blo-9 type (Plate II) has not been observed elsewhere to our knowledge. Like the elongate phytoliths that are ubiquitous to many plant taxa (Strömberg, 2003), most blocky types found in our botanical specimens of Cyperaceae were also observed in non-Cyperaceae taxa. Type Blo-1, a long (50–75 μm) acicular to oblong silica body, often infilled with black (organic?) material, was observed in the herbaceous Amaranthaceae *Celosia* spp. (Mercader et al., 2009: Fig. 5a). Types Blo-5 and Blo-8 (Plate II) were observed in several *Cyperus* species (this study and Ball, 2002), but also in 17 species of Poaceae included in our dataset (Appendix 1). Similarly, the parallelepipedal blocky type Blo-7 (Plate II) that we observed in *C. alopecuroides*, *Cyperus difformis*, and *Schoenoplectus roylei* (Appendix 1), was also observed in some woody species of the Clusiaceae, Ebenaceae, and Fabaceae families (Mercader et al., 2009: Fig. 5). In the mud samples associated to the Cyperaceae rich-environments (corresponding to the temporary Sahelian swamps and Lake Chad) we observed that "hat-shaped" Papillae type phytoliths, typical for Cyperaceae account for <3% of the total phytolith sum, even where Cyperaceae constitute mono-specific stands. In agreement with previous observations, Papillae phytoliths are poorly preserved in soils (Alexandre et al., 1997; Barboni et al., 1999; Albert et al., 2006; Finne et al., 2010). Our study shows, however, that on the contrary, blocky and elongate phytolith types may account for up to 87% of the total phytolith sum in mud samples associated to the Cyperaceae rich-environments, whereas their abundance is <31% in most samples from well-drained areas. It is worth noting that the phytolith assemblages of Cyperaceae-rich sites exhibit high percentages of elongate and blocky phytoliths, and relatively low percentages of grass silica short cells (Fig. 4). Yet, inferring the presence of Cyperaceae by the absence of evidence is hazardous. Tracing the presence of Cyperaceae in the paleoenvironments is therefore difficult.

Our study also provides new quantitative phytolith data for 35 Poaceae species including two Aristidoideae, one Arundinoideae, nine Chloridoideae, two Ehrhartoideae, and 21 Panicoideae species. Among these, *Phragmites australis* (Arundinoideae), *Cynodon dactylon* and *Dactyloctenium aegyptium* (Chloridoideae), *Leersia hexandra* and *Oryza longistaminata* (Ehrhartoideae), *Acroceras amplectens*, *Brachiaria xantholeuca*, *Cenchrus biflorus*, *Panicum anabaptistum*, *Panicum laetum*, *Panicum subalbidum*, *Pennisetum pedicellatum*, and *Setaria sphacelata* (Panicoideae) have already been studied (Piperno and Pearsall, 1998; Lu and Liu, 2003; Fahmy, 2008; Barboni and Bremond, 2009; Rossouw, 2009; Mercader et al., 2010). Quantitative and qualitative data are available for all these species (Lu and Liu, 2003; Fahmy, 2008; Barboni and Bremond, 2009; Rossouw, 2009; Mercader et al., 2010), except for *D. aegyptium* for which only semi-quantitative data are available (Piperno and Pearsall, 1998). However, the comparisons with our results are sometimes limited because descriptions and classifications of the phytolith types vary from one author to another and are more or less precise. For example, the "bilobate variant 2" category of Rossouw (2009, p. 52) includes several types of bilobates, as well as the tabular cross-shaped phytolith Cr-2 that we distinguished. The comparison is also limited with Fahmy's (2008) study, which exclusively focused on the lobate phytoliths produced by West African species of the Paniceae tribe. Fahmy's (2008) approach, however, allows some morphometric comparisons. For example, our results confirm that *C. biflorus* produces long bilobates (>25 μm); *A. amplectens* and *Panicum* spp. only produce short bilobates (≤25 μm); *Brachiaria*, *Panicum*, *Pennisetum* and *Setaria* genera produce types Bi-13 and Poly-1 (Table 3, Plate I), so-called "nodular and polylobate" (Fahmy, 2008). We believe, however, that Bi-13 and Poly-1 types cannot be used together on an assemblage as exclusive markers of genera *Brachiaria*, *Panicum*, *Pennisetum* and *Setaria* as suggested (Fahmy, 2008), because we found that such types can also be produced in small amounts by *A. amplectens*, *Hyparrhenia barteri* and *L. hexandra*. Although Fahmy (2008) found that *B. xantholeuca* and *P. pedicellatum* produce bilobates with size <20 μm and <24 μm, we found that the same species also produce large amounts of >25 μm-long bilobates (types Bi-4, -5, Plate I) (respectively 24% and 56% of the total GSSC sum). Such intra-specific variation of the bilobate size could be the result of different stages of maturity of the grass individuals, since silica accumulates in the plants from its early stage of development until its death (Sangster and Parry, 1969; Motoruma et al., 2006).

In general, our results confirm the broad pattern of phytolith production for Poaceae (Twiss et al., 1969). Poaceae produce in their epidermis a majority of GSSCs, whose diversity is impressive and difficult

to interpret (e.g. Rovner, 1971). Panicoideae and Aristidoideae species abundantly produce lobate phytoliths in their leaf epidermis, whereas most of Chloridoideae species and *Phragmites australis* (Arundinoideae) abundantly produce saddle phytoliths. Rondels are found to be very redundant in our whole grass dataset. They occur in all the grass subfamilies we studied. Large numbers of rondels (up to 95%) were observed in the genera *Eragrostis* and *Sporobolus* (Chloridoideae) in agreement with previous studies (Bamford et al., 2006; Barboni and Bremond, 2009; Mercader et al., 2010). It was surprising, however, to find up to 78% of rondels in *Leersia hexandra* (Ehrhartoideae) (Appendix 1), while previous studies mention only bilobates in this species (Barboni and Bremond, 2009; Rossouw, 2009). We found that *P. australis* produces both saddle and rondel phytoliths, in agreement with a previous study of coastal environments in southeastern USA (Lu and Liu, 2003), while some authors only observed saddles (Piperno and Pearsall, 1998; Mercader et al., 2010). Lu and Liu (2003) found that the most common rondel types produced by *P. australis* are the "two-horned towers" whereas "flat towers" rarely occur. In comparison, we found mainly conical keeled (Ro-2) and cylindrical reniform rondels (Ro-5) in our specimen of *P. australis* (Plate I, Appendix 1). Yet, all authors agree with the fact that *P. australis* abundantly produces "saddle-rondel" types (S-4). In the specimen we studied, "saddle-rondel" (S-4, Table 3) accounts for ca 39% in the total phytolith assemblage. Despite that, it would be incorrect to consider the "saddle-rondel" type as diagnostic to *P. australis* because it also occurs in small amounts (2%) in the mesophytic species *Sporobolus cordofanus* (Chloridoideae). However, our results show that the co-occurrence of the "saddle-rondel" type (S-4) with other specific types such as the conical rondels Ro-2 and Ro-6, the short-tabular bilobate Bi-7, the short-trapeziform bilobates Bi-11 and-12, and the trapeziform crosses Cr-5 and -7, indicates aquatic environments (Figs. 3 and 5).

All GSSC types that we found present in mud/soil samples from Chad, were also found present in the grass species we studied, except the rondel type Ro-8 (Plate I) with diameter ≥ 15 μm. Type Ro-8 was observed in 5/7 samples from the Sahelian region, 2/12 samples associated to the Lake Chad, and 2/7 samples from the Sudanian region. Large diameter rondels, such as Ro-8, occur in Pooideae grasses (Barboni and Bremond, 2009; Rossouw, 2009) of the temperate domain (Livingstone and Clayton, 1980). Pooideae are absent from low-altitude regions of Chad, but present in the northern Tibesti (Quézel, 1965) and the Adamawa Mountains in Cameroon (Letouzey, 1968). Phytolith input from extra-local vegetations in Lake Chad is possible through the Chari-Logone river system, which is the main supplier of current Lake Chad. These two rivers drain the humid tropics from the Central African Republic and the Adamawa Mountains in northern Cameroon (Fontes et al., 1970). Extra-local input from the northern mountains to the Sahelian and Sudanian regions is also possible by strong winds of Harmattan, which sweep Central and West Africa from the Sahara desert. Yet, a pollen study of surface mud samples from Lake Chad showed that the input of regional pollen from eolian transport is negligible (abundances of *Erica* and *Artemisia* pollen <1%) compared to the local input (Maley, 1972). Although large diameter rondels (>15 μm) may be found in the epidermis of Pooideae grasses, the most abundant phytolith types produced by those temperate grasses are trapeziform polylobates (also called "crenate") (Rossouw, 2009). We observed trapeziform polylobates in none of our mud or surface soil samples, and <4% of rondels with diameter > 15 μm in only 9 samples. We therefore believe that extra-local input of phytoliths by wind and rivers is most likely insignificant in the surface samples we analyzed.

The abundance of trees/shrubs at several local sites for which we observed a total cover of 30–40% to 60–70% is largely under-estimated by the D/P index (D/P<1). Such discrepancy was also observed for a well-preserved gallery forest in Mali (Neumann et al., 2009). Because grasses are the greatest producers of phytoliths among all living plants (Hodson et al., 2005), GSSCs may be over-represented in soils, as observed in our sample 7 (Fig. 1, Table 1), where GSSCs represent 34% of the total phytolith assemblage, although Poaceae represent less than 5% of the vegetal cover. Globular decorated phytoliths, which are considered for the D/P index (Alexandre et al., 1997; Bremond et al., 2008b) are just one among the various phytolith types produced by ligneous plants (Mercader et al., 2009). In our samples, the percentage of all ligneous indicators versus the percentage of herbaceous indicators seems to better reflect the observed tree-cover in locally closed environments than the D/P index (Fig. 4). Yet, further investigations of the phytolith signal of ligneous plants require quantitative estimates of the woody and herbaceous cover, which was not the purpose of this paper.

The regional distribution of tall grasses versus short drought-adapted grasses is well reflected by the Iph index. The Iph index does not permit, however, the discrimination of the Lake Chad herbaceous swamps from the Sudanian tall grasslands (Fig. 5). This is not surprising given that these environments are characterized by abundant Panicoideae species, which mainly produce lobate phytoliths in their leaf epidermis. The best discrimination of aquatic vegetation is obtained by the "aquatic" cohort of phytolith types, which abundance averages 42% in the mud samples, but only 23% and 14% in the samples from the Sudanian and Sahelian zones, respectively (Fig. 5). The aquatic grass signal for the Sudanian zone is higher than for the Sahelian zone, most likely because our dataset includes temporary Sudanian aquatic grasslands, for which the grass-cover evolves through the year in relation with water availability (White, 1983, Poilecot, com. pers.). To date, and to our knowledge, few studies have investigated the phytolith signal of modern lacustrine environments in Africa (Finne et al., 2010) and in the world in general (Lu and Liu, 2003; Ghosh et al., 2011). In coastal environments from North America, Lu and Liu (2003) observed that rondels are abundant in coastal wetlands in association with saddle-rondels and bilobates in smaller proportions in agreement with the abundance of *Spartina patens* (Chloridoideae), *Phragmites australis* and different species from the Panicoideae/Ehrhartoideae subfamilies in the vegetation. Although this cohort of phytoliths is comparable with the aquatic cohort of GSSCs we identified, we could not use the data summarized in the diagrams to calculate the "aquatic" index to directly compare with our results in the surface samples from Chad. Ghosh et al. (2011) found that grasses present in the mangrove swamps produce lobate phytoliths in abundance, in contrast to tidal and totally emerged mangrove which are mainly characterized by rondels. Unfortunately, little distinction was made within the main GSSC categories to allow further comparison with our results. Also, although we agree with the fact that phytoliths from all the plant parts will eventually be integrated into the soil after the plant decay, comparisons with other studies require analyzing the phytolith content of leaves, inflorescences, and roots separately. This is crucial also because leaves, roots, and inflorescences of a given species produce different phytolith assemblages (e.g. Mulholland, 1989).

Bulliform phytoliths result from the silicification of bulliform cells, which are present in the leaf epidermis of all monocot orders except the Helobiae (Beal, 1886; Metcalfe, 1960). Bulliform cells are implied in the storage of water. Under excessive heat, they allow the leaves to roll-up to reduce evapotranspiration (Moulia, 1994). Bremond et al. (2004) observed that the relative abundance of bulliform phytoliths (or Fs index) increases with increasing aridity in surface soil samples. Indeed, the calculated mean Fs index is of 10% for the Sudanian grasslands and woodlands, 17% for the Sahelian deciduous bushlands, and 35% for the Saharan steppes (>19°N) (Barboni et al., 2007). We observe the same gradient of increasing Fs index with our Chadian dataset, but Fs values are 3% for the Sudanian grasslands and woodlands, and 7% for the Sahelian deciduous bushlands and grasslands (Fig. 5). Given the homogeneous Fs signal measured in the Sudanian and Sahelian samples from West Africa, it is surprising to not obtain similar Fs values for the Chadian samples also collected in the Sudanian and Sahelian phytogeographical zones. Silicified bulliform cells may be described as regular parallelepipeds, slightly cuneiform parallelepipeds, to perfect cuneiform bodies depending on how close to the

leaf mibrid they were formed (Mauseth, 2008, pp. 194–195). As shown recently, parallelepipedal/cubic blocky phytolith types that resemble in shape and size silicified bulliform cells, may occur in diverse ligneous species of the miombo deciduous forests belonging to the Amaranthaceae, Clusiaceae, Fabaceae, or even Ebenaceae families (Mercader et al., 2009, Fig. 5). Hence, we believe that only the cuneiform blocky bodies with pronounced "fan" shapes can be confidently assigned to bulliform cells. A re-examination of the West African samples (Bremond et al., 2008a) would be necessary to check if the high Fs values really relate to high proportions of silicified bulliform phytoliths or to high proportions of non-bulliform blocky phytoliths. In our samples, the silicified cuneiform bulliform cells with pronounced fan shape (types Blo-4, -5) happen to be more abundant in the mud samples from Lake Chad herbaceous swamps (11% in average), than in the soil samples from well-drained areas of the Sahelian or Sudanian zones (3–7% in average) (Fig. 5). This is surprising given that bulliform cells are considered as xeromorphic adaptations (e.g. Esau, 1965; Fahn and Cutler, 1992; Grigore et al., 2010). In an aquatic environment such as Lake Chad, plants permanently have their roots submerged and probably suffer from less water-stress than plants from the surrounding grasslands on well-drained soils. Our results may suggest consequently that low air relative humidity which forces plant transpiration has a greater influence on the silica infilling of bulliform cells than soil water availability in the environmental context of current Lake Chad. This hypothesis is in agreement with an earlier experimental study on some British grasses that highlights the importance of a submerged root system, as well as high transpiration rate for increasing the silicification of bulliform cells (Parry and Smithson, 1964; Sangster and Parry, 1969).

6. Conclusion

Surveys of the phytoliths occurring in plants are required to find specific types that could improve the taxonomical identifications (Piperno and Pearsall, 1998; Neumann et al., 2009). Diagnostic phytolith types at the species or genus level are rare, but the number has increased since plant phytolith reference collections began (Piperno and Pearsall, 1998; Strömberg, 2003; Mercader et al., 2009; Eichhorn et al., 2010; Mercader et al., 2010). Our study on botanical specimens, which represent 11% of the Poaceae species (26% of the genera) and 6% of the Cyperaceae species (15% of the genera) reported in the Flora of Chad (César and Lebrun, 2003), did not allow the discovery of any diagnostic phytoliths for the Poaceae species, genus, or subfamily. For the Cyperaceae, however, we found that the orbicular smooth blocky type Blo-9 (Plate II) is unique to *Cyperus* species. To our knowledge, Blo-9 has not been described elsewhere. Yet, we are reluctant to label this phytolith type diagnostic for *Cyperus* given the inherent problem of phytolith redundancy.

The analysis of botanical specimens, despite being limited to 37 species allowed the investigation of the environmental signal of phytoliths for aquatic, mesophytic, and xerophytic grasses. The joint analysis of plant and soil samples contributes to better constrain the environmental and climatic signal carried by phytolith assemblages. Despite the important phytolith redundancy that we observed in the plant and soil samples from Chad, we found that it is possible to distinguish aquatic from non-aquatic environments based on the phytolith assemblages preserved in the soils. A cohort of eight grass silica short cells, including two rondel types (Ro-2 and Ro-6), one tabular and four trapeziform lobate types (Bi-7, Bi-11, Bi-12, Cr-5, and Cr-7) and the "saddle-rondel" (S-4), which occur preferentially in aquatic grasses, also occur in abundance in mud samples from permanent and temporary water-bodies in Chad. On the contrary, this cohort of grass phytoliths is little represented in the samples from well-drained soils. Despite the abundance of sedges in some aquatic environments, and the abundance of Papillae phytoliths in their epidermis, the presence and abundance of Cyperaceae are difficult to trace because Papillae phytoliths are poorly preserved in the soils.

In conclusion, our study demonstrates that by exploiting the great morphological diversity of GSSCs present in the Lake Chad phytolith assemblages, it is possible to segregate the aquatic vegetation zones from the non-aquatic grasslands and woodlands, and therefore improve paleoclimatic and paleoenvironmental reconstructions, notably at hominin sites in Chad.

Supplementary related to this article can be found online at doi:10.1016/j.revpalbo.2012.03.010.

Acknowledgments

We thank the Chadian Authorities (Ministère de l'Education Nationale de l'Enseignement Supérieur et de la Recherche, University of Ndjamena, CNAR), the Ministère Français de l'Enseignement Supérieur et de la Recherche (UFR SFA, University of Poitiers, CNRS-INEE, ANR, Project ANR-09-BLAN-0238, PI's Michel Brunet), the Ministère Français des Affaires Etrangères et Européennes (DCSUR Paris and French Embassy in Ndjamena, Chad; FSP, Project no. 2005-54 of the Franco-Chadian cooperation) and the Région Poitou-Charentes for financial support. We also thank Dr. M. Abderamane (University of Ndjamena) and M. Adoum (CNAR) for collecting the samples at Bol. We are also grateful to J. Maley (ISEM) and I. de Zborowski (CIRAD) for fruitful discussions regarding Chad vegetation and to G. Florent, C. Noël and J. Surault for administrative guidance of the general project. We thank the editor M. Sephenson, K. Neumann, and another anonymous reviewer for their comments and suggestions to improve our manuscript.

References

Albert, R.M., Bamford, M.K., Cabanes, D., 2006. Taphonomy of phytoliths and macroplants in different soils from Olduvai Gorge (Tanzania) and the application to Plio–Pleistocene palaeoanthropological samples. Quaternary International 148, 78–94.

Alexandre, A., Meunier, J.-D., Lézine, A.-M., Vincens, A., Schwartz, D., 1997. Phytoliths: indicators of grassland dynamics during the late Holocene in intertropical Africa. Palaeogeography, Palaeoclimatology, Palaeoecology 136, 213–229.

Ball, T.B., 2002. Phytoliths of Dhofar, Oman, Arabia, CD-ROM, Brigham Young University, Provo, UT.

Bamford, M.K., Albert, R.M., Cabanes, D., 2006. Plio–Pleistocene macroplant fossil remains and phytoliths from Lowermost Bed II in the eastern palaeolake margin of Olduvai Gorge, Tanzania. Quaternary International 148, 95–112.

Barboni, D., Bremond, L., 2009. Phytoliths of East African grasses: an assessment of their environmental and taxonomic significance based on floristic data. Review of Palaeobotany and Palynology 158, 29–41.

Barboni, D., Bonnefille, R., Alexandre, A., Meunier, J.D., 1999. Phytoliths as paleoenvironmental indicators, West Side Middle Awash Valley, Ethiopia. Palaeogeography, Palaeoclimatology, Palaeoecology 152, 87–100.

Barboni, D., Bremond, L., Bonnefille, R., 2007. Comparative study of modern phytolith assemblages from inter-tropical Africa. Palaeogeography, Palaeoclimatology, Palaeoecology 246, 454–470.

Beal, W.J., 1886. The bulliform or hygroscopic cells of grasses and sedges compared. Botanical Gazette XI, 319–326.

Blondel, C., Merceron, G., Andossa, L., Taisso, M. Hassane, Vignaud, P., Brunet, M., 2010. Dental mesowear analysis of the late Miocene Bovidae from Toros-Menalla (Chad) and early hominid habitats in Central Africa. Palaeogeography, Palaeoclimatology, Palaeoecology 292, 184–191.

Boughey, A.S., 1957. The physionomic delimitation of west african vegetation types. Journal of the West African Science Association 3, 148–165.

Bremond, L., Alexandre, A., Peyron, O., Guiot, J., 2004. Grass water stress estimated from phytoliths in West Africa. Journal of Biogeography 31, 1–17.

Bremond, L., Alexandre, A., Hély, C., Guiot, J., 2005. A phytolith index as a proxy of tree cover density in tropical areas: calibration with Leaf Area Index along a forest-savanna transect in southeastern Cameroon. Global and Planetary Change 45, 277–293.

Bremond, L., Alexandre, A., Peyron, O., Guiot, J., 2008a. Definition of grassland biomes from phytoliths in West Africa. Journal of Biogeography 35, 2039–2048.

Bremond, L., Alexandre, A., Wooller, M.J., Hély, C., Williamson, D., Schäfer, P.A., Majule, A., Guiot, J., 2008b. Phytolith indices as proxies of grass subfamilies on East African tropical mountains. Global and Planetary Change 61, 209–224.

Brunet, M., Beauvilain, A., Coppens, Y., Heintz, E., Moutaye, A.H.E., Pilbeam, D., 1995. The first australopithecine 2500 kilometres west of the Rift Valley (Chad). Nature 378, 273–275.

Brunet, M., Beauvilain, A., Geraads, D., Guy, F., Kasser, M., Mackaye, H.T., Maclatchy, M.L., Mouchelin, G., Sudre, J., Vignaud, P., 1996. *Australopithecus bahrelghazali*, une nouvelle espèce d'Hominidé ancien de la région de Koro Toro (Tchad). Comptes Rendus de l'Académie des Sciences de Paris Série IIa 322, 907–913.

Brunet, M., Guy, F., Pilbeam, D., Mackaye, H.T., Likius, A., Ahounta, D., Beauvilain, A., Blondel, C., Bocherensk, H., Boisserie, J.-R., de Bonis, L., Coppens, Y., Dejax, J., Denys, C., Duringer, P., Eisenmann, V., Fanone, G., Fronty, P., Geraads, D., Lehmann, T., Lihoreau, F., Louchart, A., Mahamat, A., Merceron, G., Mouchelin, G., Otero, O., Pelaez-Campomanes, P., De Leon, M.Ponce, Rage, J.-C., Sapanetk, M., Schuster, M., Sudre, J., Tassy, P., Valentin, X., Vignaud, P., Viriot, L., Zazzo, A., Zollikofer, C., 2002. A new hominid from the Upper Miocene of Chad, Central Africa. Nature 418, 145–151.

Brunet, M., Guy, F., Pilbeam, D., Lieberman, D.E., Likius, A., Mackaye, H.T., de Léon, M.S. Ponce, Zollikofer, C.P.E., Vignaud, P., 2005. New material of the earliest hominid from the Upper Miocene of Chad. Nature 434, 752–755.

César, J., Lebrun, J.-P., 2003. Flore du Tchad. Laboratoire de Recherches Vétérinaires et Zootechniques de Farcha, N'Djaména.

Coppens, Y., Koeniguer, J.C., 1976. Sur les flores ligneuses disparues Plio-Quaternaires du Tchad et du Niger. Comptes Rendus de l'Académie des Sciences de Paris 265, 1282–1285.

Diester-Haass, L., Sehrader, H.T., Thiede, T., 1973. Sedimentological and paleoclimatological investigations of two pelagic ooze cores off Cape Barbas, North-West Africa. Meteor Forschungs-Ergebnisse Reihe C 16, 19–66.

Eichhorn, B., Neumann, K., Garnier, A., 2010. Seed phytoliths in West African Commelinaceae and their potential for palaeoecological studies. Palaeogeography, Palaeoclimatology, Palaeoecology 298, 300–310.

Ellis, R.P., 1979. A procedure for standardizing comparative leaf anatomy in the Poaceae. II. The epidermis as seen in surface view. Bothalia 12, 641–671.

Esau, K., 1965. Plant Anatomy. John Wiley and Sons, New York. 767 pp.

Fahmy, A.G., 2008. Diversity of lobate phytoliths in grass leaves from the Sahel region, West tropical Africa: tribe Paniceae. Journal of Plant Systematics and Evolution 270, 1–23.

Fahn, A., Cutler, D.F., 1992. Xerophytes, Handbuch der Pflanzenanatomie (band XIII, teil 3). Gebrüder Borntraeger, Berlin, Stuttgart.

Finne, M., Norstrom, E., Risberg, J., Scott, L., 2010. Siliceous microfossils as late-Quaternary paleo-environmental indicators at Braamhoek wetland, South Africa. The Holocene 20, 747–760.

Fontes, J.C., Maglione, G., Roche, M.A., 1970. Eléments d'hydrologie isotopique dans le bassin du lac Tchad. In Peaceful Uses of Atomic Energy in Africa. International Atomic Energy Agency, Vienne, pp. 209–219.

Fotius, G., Lemoalle, J., 1976. Reconnaissance de l'évolution de la végétation du Lac Tchad entre janvier 1974 et juin 1976. Office de la recherche scientifique et technique outre-mer, N'Djaména.

Fredlund, G.G., Tieszen, L.T., 1994. Modern phytolith assemblages from the North American Great Plains. Journal of Biogeography 21, 321–335.

Gaston, A., 1996. Agropastoralisme. Centre de Coopération Internationale en Recherche Agronomique, Elevage et Médecine Véterinaire Tropicale. : Atlas d'Elevage du Bassin du Lac Tchad. Centre Technique de Coopération Agricole et Rurale, Waganingen, pp. 39–55.

Gaston, A., Dulieu, D., 1976. Pâturages naturels du Tchad. Département d'Elevage et Médecine Vétérinaire des Pays Tropicaux, Maison Alfort.

Ghosh, R., Naskar, M., Bera, S., 2011. Phytolith assemblages of grasses from the Sunderbans, India and their implications for the reconstruction of deltaic environments. Palaeogeography, Palaeoclimatology, Palaeoecology 311, 93–102.

Grigore, M.-N., Toma, C., Boscaiu, M., 2010. Ecological implications of bulliform cells on halophytes, in salt and water stress natural conditions. Scientific Annals of Alexandru Ioan Cuza University of Iasi. New Series, Section 2. Vegetal Biology 56, 5–15.

Hodson, M.J., White, P.J., Mead, A., Broadley, M.R., 2005. Phylogenetic variation in silicon composition of plants. Annals of Botany 96, 1027–1046.

Kellogg, E.A., 2001. Evolutionary history of the grasses. Plant Physiology 125, 1198–1205.

Kondo, R., Childs, C., Atkinson, I., 1994. Opal Phytoliths of New Zealand. Manaaki Whenua Press, Lincoln. 85 pp.

Lebart, L., Morineau, A., Piron, M., 2000. Statistique Exploratoire Multidimensionnelle. Dunod, pp. 181–184. ed.

Lebatard, A.-E., Bourlès, D.L., Duringer, P., Jolivet, M., Braucher, R., Carcaillet, J., Schuster, M., Arnaud, N., Monié, P., Lihoreau, F., Likius, A., Mackaye, H.T., Vignaud, P., Brunet, M., 2008. Cosmogenic nuclide dating of *Sahelanthropus tchadensis* and *Australopithecus bahrelghazali*: Mio–Pliocene hominids from Chad. Proceedings of the National Academy of Sciences 105, 3226–3231.

Lebatard, Anne-Elisabeth, Bourlès, Didier L., Braucher, Régis, Arnold, Maurice, Duringer, Philippe, Jolivet, Marc, Moussa, Abderamane, Deschamps, Pierre, Roquin, Claude, Carcaillet, Julien, Schuster, Mathieu, Lihoreau, Fabrice, Likius, Andossa, Mackaye, Hassan Taisso, Vignaud, Patrick, Brunet, Michel, 2010. Application of the authigenic 10Be/9Be dating method to continental sediments: reconstruction of the Mio–Pleistocene sedimentary sequence in the early hominid fossiliferous areas of the northern Chad Basin. Earth and Planetary Science Letters 297, 57–70.

LeFur, S., Fara, E., Mackaye, H.T., Vignaud, P., Brunet, M., 2009. The mammal assemblage of the hominid site TM266 (Late Miocene, Chad Basin): ecological structure and paleoenvironmental implications. Naturwissenschaften 96, 565–574.

Lemoalle, J., Hourtal, D., 1996. Eaux de surface. Centre de Coopération Internationale en Recherche Agronomique, Elevage et Médecine Véterinaire Tropicale. : Atlas d'Elevage du Bassin du Lac Tchad. Centre Technique de Coopération Agricole et Rurale, Wageningen, pp. 23–28.

Letouzey, R., 1968. Etude phytogéographique du Cameroun. Encyclopedia biologica n°69. Paul Lechevalier, Paris, p. 511.

Lézine, A.-M., Watrin, J., Vincens, A., Hély, C., 2009. Are modern pollen data representative of west African vegetation? Review of Palaeobotany and Palynology 156, 265–276.

Livingstone, D.A., Clayton, W.D., 1980. An altitudinal cline in tropical African grass floras and its paleoecological significance. Quaternary Research 13, 392–402.

Lu, H., Liu, K., 2003. Phytoliths of common grasses in the coastal environments of southeastern USA. Estuarine, Coastal and Shelf Science 58, 587–600.

Madella, M., Alexandre, A., Ball, T., 2005. International Code for Phytolith Nomenclature 1.0. Annals of Botany 96, 253–260.

Maley, J., 1972. La sédimentation pollinique actuelle dans la zone du lac Tchad (Afrique Centrale). Pollen et Spores 14, 263–307.

Mauseth, J.D., 2008. In: Crowley, A., Williams, R., Faust, L., Kenney, L. (Eds.), Plant Anatomy. Blackburn Press, Caldwell. 576 pp.

Mercader, J., Bennett, T., Esselmont, C., Simpson, S., Walde, D., 2009. Phytoliths in woody plants from the Miombo woodlands of Mozambique. Annals of Botany 104, 91–113.

Mercader, J., Astudillo, F., Barkworth, M., Bennett, T., Esselmont, C., Kinyanjui, R., Grossman, D.L., Simpson, S., Walde, D., 2010. Poaceae phytoliths from the Niassa Rift, Mozambique. Journal of Archaeological Science 1953–1967.

Metcalfe, C.R., 1960. Anatomy of the monocotyledons. In: Metcalfe, C.R. (Ed.), Anatomy of the Monocotyledons. Clarendon Press, Oxford. 731 pp.

Motoruma, H., Fujii, T., Suzuki, M., 2006. Silica deposition in abaxial epidermis before the opening of leaf blades of *Pleioblastus chino* (Poaceae, Bambusoideae). Annals of Botany 97, 513–519.

Moulia, B., 1994. The biomechanics of leaf rolling. Biomimetics 2, 267–281.

Mulholland, S.C., 1989. Phytolith shape frequencies in North Dakota grasses: a comparison to general patterns. Journal of Archaeological Science 16, 489–511.

Mulholland, S.C., Rapp, G., 1992. A morphological classification of grass silicabodies. In: Rapp, G., Mulholland, S.C. (Eds.), Phytolith Systematics. Plenum, New York, pp. 65–89.

Neumann, K., Fahmy, A., Lespez, L., Ballouche, A., Huysecom, E., 2009. The Early Holocene palaeoenvironment of Ounjougou (Mali): phytoliths in a multiproxy context. Palaeogeography, Palaeoclimatology, Palaeoecology 276, 87–106.

Olivry, J.-C., Chouret, A., Vuitlaume, G., Lemoalle, J., Bricquet, J.-P., 1996. Hydrologie du lac Tchad. Institut Français de Recherche Scientifique pour le Développement en Coopération, Paris.

Ollendorf, A.L., 1992. Toward a classification scheme of sedge (Cyperaceae) phytoliths. In: Rapp Jr., G., Mulholland, S.C. (Eds.), Phytolith Systematics. Plenum Press, New York.

Ollendorf, A.L., Mulholland, S.C., Rapp Jr., G., 1987. Phytolith from Israeli sedges. Israel Journal of Botany 36, 125–132.

Ollendorf, A.L., Mulholland Jr., S.C., Rapp, G., 1988. Phytolith analysis as a means of plant identification: *Arundo donax* and *Phragmites communis*. Annals of Botany 61, 209–214.

Otero, O., Pinton, A., Mackaye, H.T., Likius, A., Vignaud, P., Brunet, M., 2010. The fish assemblage associated with the Lare Miocene Chadian hominid (Toros-Menalla, Western Djurab) and its palaeoenvironmental significance. Palaeontographica, Abteilung A: Palaeozoology, Stratigraphy 292, 21–51.

Palmer, P.G., Gerbeth-Jones, S., Hutchison, S., 1985. A Scanning Electron Microscope Survey of the Epidermis of East African Grasses, III. Smithsonian Contributions to Botany, Washington. 136 pp.

Parry, D.W., Smithson, F., 1964. Types of opaline silica depositions in the leaves of British grasses. Annals of Botany 28, 169–185.

Piperno, D.R., 1988. Phytolith Analysis — An Archaeological and Geological Perspective. Academic Press (Harcourt Brace Jovanovich), New York. 280 pp.

Piperno, D.R., 2006. Phytoliths. A Comprehensive Guide for Archaeologists and Paleoecologists. AltaMira Press, Oxford. (Rowman & Littlefield).

Piperno, D.R., Pearsall, D.M., 1998. The silica bodies of tropical American grasses: morphology, taxonomy, and implications for grass systematics and fossil phytolith identification. Smithsonian Contribution to Botany 85, 1–40.

Poilecot, P., 1999. Les Poaceae du Niger. Centre de Coopération Internationale en Recherche Agronomique, Conservatoire et Jardins botaniques de Genève, Union Internationale pour la Conservation de la Nature, vol. 56. Boissiera, Genève, p. 766.

Quézel, P., 1965. La végétation du Sahara. Du Tchad à la Mauritanie. Geobotanica Selecta, 2. Gustaf Fisher Verlag, Stuttgart, p. 333.

Rossouw, L., 2009. The application of fossil grass-phytolith analysis in the reconstruction of late Cenozoic environments in the South African interior, PhD Thesis. Bloemfontein: University of the Free State.

Rovner, I., 1971. Potential of opal phytoliths for use in paleoecological reconstruction. Quaternary Research 1, 343–359.

Runge, F., 1999. The opal phytolith inventory of soils in central Africa — quantities, shapes, classification, and spectra. Review of Palaeobotany and Palynology 107, 23–53.

Sangster, A.G., Parry, D.W., 1969. Sorne factors in relation to bulliforrn cell silicification in the grass leaf. Annals of Botany 33, 315–323.

Schmidt, M., Thiombiano, A., Zizka, A., König, K., Brunken, U., Zizka, G., 2011. Patterns of plant functional traits in the biogeography of West African grasses (Poaceae). African Journal of Ecology 49, 490–500.

Schuster, M., 2002. Sédimentologie et paléoécologie des séries à vertébrés du paléolac Tchad depuis le Miocène supérieur, PhD Thesis. Strasbourg: Université Louis-Pasteur.

Schwartz, D., Mariotti, A., 1996. Le delta13C des principales graminées et cypéracées du Congo, conséquences pour les études isotopiques des savanes et forêts d'Afrique centrale, Dynamique à long terme des écosystèmes forestiers intertropicaux.

Centre National de la Recherche Scientifique, Office de la Recherche Scientifique et Technique Outre-Mer, Paris, pp. 89–92.
Scurfield, G., Anderson, A., Segnit, E.R., 1974. Silica in woody stems. Anatomical Journal of Botany 22, 211–229.
Strömberg, C. A. E., 2003. The origin and spread of grass-dominated ecosystems during the Tertiary of North America and how it relates to the evolution of hypsodonty in equids, PhD Thesis, Integrative Biology. Berkeley: University of California.
Thorn, V.C., 2004. An Annotated Bibliography of Phytolith Analysis and Atlas of Selected New Zealand Subantarctic and Subalpine Phytoliths Antarctic Data Series, 29, pp. 1–67.
Twiss, P.C., Suess, E., Smith, R.M., 1969. Morphology classification of grass phytoliths. Soil Science Society of America 33, 109–115.
UNEP, United Nations Environment Programme, 2004. Lake Chad Basin, Global International Waters Assessment.
Vignaud, P., Duringer, P., Mackaye, H.T., Likius, A., Blondel, C., Boisserie, J.-R., de Bonis, L., Eisenmann, V., Etienne, M.-E., Geraads, Denis, Guy, F., Lehmann, T., Lihoreau, F., Lopez-Martinez, N., Mourer-Chauviré, C., Otero, O., Rage, J.-C., Schuster, M., Viriot, L., Zazzo, A., Brunet, M., 2002. Geology and palaeontology of the Upper Miocene Toros-Menalla hominid locality, Djurab Desert, Northern Chad. Nature 418, 152–155.
Wallis, L., 2003. An overview of leaf phytolith production patterns in selected northwest Australian flora. Review of Palaeobotany and Palynology 125, 201–248.
Watson, L., Dallwitz, M. J., 1992 onwards. GrassBase — the grass genera of the world: descriptions, illustrations, identification, and information retrieval; including synonyms, morphology, anatomy, physiology, phytochemistry, cytology, classification, pathogens, world and local distribution, and references. Available at: http://delta-intkey.com/grass/ (accessed January 2012).
White, F., 1983. The Vegetation Map of Africa, Recherches sur les ressources naturelles. Office de la Recherche Scientifique et Technique Outre-Mer, United Nations Educational, Scientific and Cultural Organization, Paris. 384.
WoldeGabriel, G., Ambrose, S.H., Barboni, D., Bonnefille, R., Bremond, L., Currie, B., DeGusta, D., Hart, W.K., Murray, A.M., Renne, P.R., Jolly-Saad, M.C., Stewart, K.M., White, T.D., 2009. The geological, isotopic, botanical, invertebrate, and lower vertebrate surroundings of *Ardipithecus ramidus*. Science 326, 65e61–65e65.
Zazzo, A., Bocherens, H., Brunet, M., Beauvilain, A., Billiou, D., Mackaye, H.T., Vignaud, P., Mariotti, A., 2000. Herbivore paleodiet and paleoenvironmental changes in Chad during the Pliocene using stable isotope ratios of tooth enamel carbonate. Paleobiology 26, 294–309.